REPORT DOCUMENTATION PAGE

Form Approved OMB No. 074-0188

1. AGENCY USE ONLY (Leave blank)	2. REPORT DATE 12/4/96	3. REPORT TYPE AND DATES COVERED Technical Report

4. TITLE AND SUBTITLE

Desalination with Carbon Aerogel Electrodes

5. FUNDING NUMBERS

DOE
LLNL Contract No. W-7405-Eng-48.

6. AUTHOR(S)

J.C. Farmer, J.H. Richardson, D.V. Fix, S.L. Thomson, & S.C. May

7. PERFORMING ORGANIZATION NAME(S) AND ADDRESS(ES)

Chemistry and Material Science Department
Lawrence Livermore National Laboratory
Livermore, CA 94551

Bechtel Technology and Consulting
Bechtel National Corporation
San Francisco, CA 94119

8. PERFORMING ORGANIZATION REPORT NUMBER

LLNL
Report No. UCRL-ID-125298 Rev. 1

9. SPONSORING / MONITORING AGENCY NAME(S) AND ADDRESS(ES)

SERDP
901 North Stuart St. Suite 303
Arlington, VA 22203

10. SPONSORING / MONITORING AGENCY REPORT NUMBER

N/A

11. SUPPLEMENTARY NOTES

Information available through the Lawrence Livermore National Laboratory, Report No. UCRL-ID-125298 Rev. 1, 4 December 1996. This work was supported in part by DOE under LLNL Contract No. W-7405-Eng-48.

12a. DISTRIBUTION / AVAILABILITY STATEMENT

Approved for public release: distribution is unlimited

12b. DISTRIBUTION CODE

A

13. ABSTRACT ***(Maximum 200 Words)***

An electrically-regenerated electrosorption process known as carbon aerogel CDI has been developed by Lawrence Livermore National Laboratory (LLNL) for continuously removing ionic impurities from aqueous streams. A salt solution flows in an unobstructed channel formed by numerous pairs of parallel carbon aerogel electrodes. Each electrode has a very high BET surface area and very low electrical resistivity. BET surface areas of 1.3×10^7 ft^2 lb^{-1} have been achieved with thermal activation. After polarization, anions and cations are removed from the electrolyte by the imposed electric field and electrosorbed onto the carbon aerogel. The solution is thus separated into two streams, concentrate and purified water. Based upon this analysis, it is concluded that carbon aerogel CDI may be an energy-efficient alternative to electrodialysis and reverse osmosis for the desalination of brackish water ($\leq$ 5000 ppm), provided that the cell geometries and aerogel properties are carefully tailored for such applications.

14. SUBJECT TERMS

Aerogel, electrosorption, Desalination, SERDP

15. NUMBER OF PAGES

59

16. PRICE CODE N/A

17. SECURITY CLASSIFICATION OF REPORT	18. SECURITY CLASSIFICATION OF THIS PAGE	19. SECURITY CLASSIFICATION OF ABSTRACT	20. LIMITATION OF ABSTRACT
unclass.	unclass.	unclass.	UL

Lawrence Livermore National Laboratory Report No. UCRL-ID-125298 Rev. 1

Desalination with Carbon Aerogel Electrodes

Joseph C. Farmer, Jeffrey H. Richardson and David. V. Fix
Chemistry and Materials Science Department
Lawrence Livermore National Laboratory
Livermore, California 94550

Scott L. Thomson and Sherman C. May
Bechtel Technology and Consulting
Bechtel National Corporation
San Francisco, California 94119

December 4, 1996

Abstract

An electrically-regenerated electrosorption process known as carbon aerogel CDI has been developed by Lawrence Livermore National Laboratory (LLNL) for continuously removing ionic impurities from aqueous streams. A salt solution flows in an unobstructed channel formed by numerous pairs of parallel carbon aerogel electrodes. Each electrode has a very high BET surface area (2.0-5.4x10^6 ft^2 lb^{-1} or 400-1100 m^2 g^{-1}) and very low electrical resistivity ($\leq$ 40 mΩ cm). BET surface areas of 1.3x10^7 ft^2 lb^{-1} (2600 m^2 g^{-1}) have been achieved with thermal activation. After polarization, anions and cations are removed from the electrolyte by the imposed electric field and electrosorbed onto the carbon aerogel. The solution is thus separated into two streams, concentrate and purified water. Based upon this analysis, it is concluded that carbon aerogel CDI may be an energy-efficient alternative to electrodialysis and reverse osmosis for the desalination of brackish water ($\leq$ 5000 ppm), provided that cell geometries and aerogel properties are carefully tailored for such applications. The intrinsic energy required by this process is approximately $QV/2$, where Q is the stored electrical charge and V is the voltage between the electrodes, plus losses due to parasitic electrochemical reactions, electrical resistance and pressure drop. The estimated requirement for desalination of a 2000 ppm feed is estimated to be ~0.53-2.5 Wh gal^{-1} (0.50-2.4 kJ L^{-1}), depending upon voltage, flow rate, cell dimensions, carbon aerogel density, recovery ratio and other parameters. These estimates assume that 50-70% of the stored electrical energy is reclaimed during regeneration (electrical discharge). The possibility of such low power requirements for desalination of brackish water (BW), as well as the possibility of energy storage and recovery, may make this process attractive for such applications. Though the intrinsic energy requirement for desalination of sea water (SW) are also relatively low, this application will be much more difficult. Additional work will be required to determine the suitability of carbon aerogel CDI for desalination of streams that contain more than 5000 ppm total dissolved solids (TDS). Applications at 2000 ppm will require the construction of electrochemical cells with extremely tight, demanding tolerances. At the present time, the process is best suited for streams with relatively dilute impurities, as recently demonstrated during a field test at LLNL Treatment Facility C.

Introduction

Background. Throughout time man has used fresh water for drinking, industrial, and agricultural purposes, and has settled where suitable water was available, as stated by Summers [1]. Progressive industrialization and expansion of irrigation agriculture add to the ever increasing use of fresh water. The rapid increase of the global population and the non-uniform distribution of fresh water around the world has motivated research into the development of various desalination methods. If pure water could be economically obtained from SW, it would have a dramatic affect on our future standard of living, as competition for fresh water increases. President John F. Kennedy said, "If we could ever competitively, at a cheap rate, get fresh water from salt water, ... this would be in the long-range interests of humanity, ... (and) would dwarf any other scientific accomplishment." Desalination of SW and BW offers great potential for increasing the availability of fresh water. The concentration of salt in SW is typically 35,000 ppm, though it may reach 50,000 ppm in some areas. The concentration of salt in BW rarely exceeds 10,000 ppm, while most BWs in California have concentrations between 800 and 3200 ppm. These levels must be reduced to less than 500 ppm for drinking water. In some cases, lower product concentrations are required for agricultural applications. Until now, we have been paying a low price for fresh water, however the cost may increase dramatically as demand increases and we are forced to use other methods to avail ourself of fresh water.

Desalination Processes

Desalination Options. Most large-scale desalination processes in the world are based on variations of evaporation and distillation. These energy-intensive, thermal processes require heat that is derived from burning fossil or nuclear fuel. Despite the huge energy requirements, thermal processes are favored for SW desalination since large production rates are possible with reasonable investments in capital equipment. Electrodialysis (ED), electrodialysis reversal (EDR) and reverse osmosis (RO) systems are more energy efficient, but require expensive and troublesome membranes. Membranes are plagued by chemical degradation, biological fouling and inorganic scale formation problems, and must be periodically replaced. Membrane processes have been used for desalination of SW, but are more often considered for the desalination of reservoirs of brackish water (BW). In some cases, capacitive deionization (CDI) with carbon aerogel electrodes may serve as an energy-efficient alternative to thermal and membrane desalination processes. Carbon aerogel is an ideal electrode material because of its low electrical resistivity ($\leq$ 40 mΩ cm), high specific surface area (2.0-5.4x10^6 ft^2 lb^{-1} or 400-1100 m^2 g^{-1}), controllable pore size distribution ($\leq$ 50 nm), and monolithic structure. Note that surface areas as high as 1.3x10^7 ft^2 lb^{-1} (2600 m^2 g^{-1}) have been achieved with activation.

Thermal Processes. Thermal processes are the oldest and most commonly used methods of desalination in the world. The thermal efficiency of such a process is usually called the "performance ratio" or "economy" and is usually defined as the pounds of distillate produced per 1000 Btu of heat input. Here, the total required energy (electrical and thermal) is given in units of Wh gal^{-1} (kJ L^{-1}). Evaporative distillation serves as the major source of fresh water in the Middle East. Early designs are of the submerged-tube, multiple-effect type. In such systems,

steam is fed through tubes submerged in a stagnant pool of brine, thereby causing the brine to boil. Evaporated water is condensed as pure, salt-free water. Salts remain in the brine phase, which becomes more concentrated. Energy recovery is accomplished by heat transfer from the product to the feed. Scale formation on heat transfer surfaces lowers the thermal efficiency of the process and is exacerbated by high operating temperatures, which leads to localized supersaturation and precipitation. Multistage flash evaporation (MSF) is an alternative thermal process that was developed to improve process efficiency and to minimize operating problems associated with scale formation. Since the introduction of MSF in the 1960's, about 56% of the total installed desalination plant capacity has been MSF [2]. In this process, salt water is introduced into a low pressure chamber where it undergoes flash evaporation. Note that vapor can be produced from a liquid at its boiling point by adding heat at constant pressure and temperature (boiling), or by reducing pressure at constant temperature (flashing). The amount of heat that is lost from the process is minimized by using several counter-current stages, each at a lower temperature and pressure than the preceeding stage. Energy recovery is improved by adding stages. Since heat transfer surfaces in MSF processes are maintained at lower temperatures than those in submerged-tube multiple-effect systems, problems associated with scale formation are less. A typical MSF system consumes ~320 Wh gal^{-1} (304 kJ L^{-1}) for SW desalination, compared to the theoretical minimum given here of ~2.0 Wh gal^{-1} (1.9 kJ L^{-1}). Note that a simple evaporator without energy recovery would require more than 2720 Wh gal^{-1} (2587 kJ L^{-1}). Energy recovery can be enhanced by using mechanical vapor recompression (MVC). Mechanical compression is used to elevate the temperature of vapor from the evaporator to a point where it can be used to drive the evaporator. The hot compressed vapor loses its latent heat to the incoming feed and condenses, yielding salt-free product. Since the temperature differential between the hot and cold side of the heat transfer surface is only 7-9 °F (4-5 °C), the required energy and rates of scale formation are both low. A typical MVC system consumes ~30-41 Wh gal^{-1} (29-39 kJ L^{-1}). See Table 1 for published energy requirements for SW desalination processes [2].

Reverse Osmosis. Reverse osmosis (RO) is a separation processes which uses membranes to selectively remove water from a salt solution. In conventional osmosis, water or solvent flows through a semipermeable membrane from a less concentrated solution to an area of higher concentration. This normal osmotic flow can be reversed by applying pressure in excess of the osmotic pressure. The flow through the semipermeable membrane is governed by Equation 1:

$$F_w = A(\Delta p - \Delta \pi) \qquad [1]$$

where F_w is the water flux (g cm^{-2} s^{-1}), A is the water permeability constant (g cm^{-2} s^{-1} atm^{-1}), Δp is the differential pressure applied across the membrane (atm), and $\Delta \pi$ is the osmotic pressure differential across the membrane (atm) [3a]. The osmotic pressure is a function of salt concentration and is represented by Equation 2:

$$\Delta \pi = 1.12(T + 273)\sum_j m_j \qquad [2]$$

where $\Delta\pi$ is the osmotic pressure (psi), T is the temperature (°C), and m_i is the molality of the i-th ionic or non-ionic constituent [3b]. A rule of thumb that works well with natural water, based on NaCl, is that the osmotic pressure increases by approximately 0.01 psi (6.8×10^{-4} atm) for each ppm (mg L^{-1}) increase in salt concentration. Applying this rule to SW, the osmotic pressure is estimated to be about 350 psi (24 atm). The salt flow through a semipermeable membrane can be expressed by Equation 3:

$$F_s = B(C_1 - C_2) = B\Delta C \qquad [3]$$

where B is the salt permeability constant (cm s^{-1}) and $\Delta C = C_1 - C_2$ is the concentration gradient across the membrane (g cm^{-3}) [3a]. RO with cellulose acetate, polyamide or other polymer semipermeable membranes can be used to desalinate BW or SW. Usually, membranes are incorporated into plate-and-frame, tubular, or spiral-wound modular units. An RO-based desalination process usually consists of several of these modules connected together in series-parallel arrays. The processed feedwater is separated into two streams, permeate and brine. The permeate passes through the membranes due to the pressure gradient while the brine is continuously rejected. Typical systems reject brine with a salt concentration of two to four times (2X to 4X) greater than that of the feed. Since mechanical energy is used in lieu of heat energy, RO systems operate at ambient temperature and avoid some of the problems associated with high-temperature thermal processes. RO systems do suffer from problems such as concentration polarization, chemical degradation, biological fouling, and scaling of membranes. Concentration polarization at the brine-membrane interface increases the mass transfer resistance and requires additional pressure to overcome. Furthermore, it causes localized supersaturation and precipitation, which exacerbates scale formation. As pores in the membrane become blocked, the flux of water at a constant applied pressure will reduce. In order to avoid such problems, feed water must be pretreated. RO systems are generally classified as sea water (800-1500 psi), standard pressure (400-650 psi), low pressure (200-300 psi) and nanofiltration (45-150 psi) [3a,3b]. Estimates of the osmotic pressure, membrane pressure, and minimum possible energy requirement for desalination of feed streams with 1000-35,000 ppm TDS are found in Table 2. These estimates are based upon heuristic guidelines. A typical RO system requires ~25-36 Wh gal^{-1} (24-34 kJ L^{-1}) for desalination of SW, depending upon the use of energy recovery, whereas a low-pressure RO system requires ~8.5 Wh gal^{-1} (8.1 kJ L^{-1}) for desalination of BW with 1630 ppm TDS [2,4]. Extremely large RO plants have been built and successfully operated. For example, the Yuma Desalting Plant in Yuma, Arizona is the largest RO facility in the world and is operated by the U.S. Department of Interior, Bureau of Reclamation. Construction of this plant was authorized by the Colorado River Basin Salinity Control Act (PL 93-320), legislation passed by the U.S. Congress in 1977. The objective of this monumental project is to enable the United States to satisfy conditions of a treaty with Mexico (Treaty TS 994, 1944; Ammended with Minute No. 242, 1977). Under that agreement, the United States agreed that the salinity of water delivered to Mexico at Morelos Dam would not exceed the salinity level at the Imperial Dam by more than 115±39 ppm. The Imperial Dam is 27 miles (43 km) upstream of the Morelos Dam. The Yuma Desalting Plant uses cellulose acetate RO membranes to desalinate as much as 72.4×10^6 gal d^{-1} (275×10^6 L d^{-1}) of saline drainage water from farmlands east of Yuma. The salt concentration is lowered from ~3000 to ≤ 300 ppm with a differential pressure of ~362 psi (25

atm). The product (~300 ppm) and unprocessed drainage water (~3000 ppm) are blended and sent to the Colorado River, while concentrated brine (~10,000 ppm) is rejected and sent to the Santa Clara Marsh at the Gulf of California. This RO-based desalination plant enables the United States to salvage drainage water that otherwise would be too saline to deliver to Mexico, thereby saving up to 78,500 acre-feet (97×10^6 m^3) of Colorado River water per year. The Yuma Desalting Plant is not being operated at the present time since water quality requirements can be temporarily met without it. It remains in a *state of readiness*.

Electrodialysis. In a conventional electrodialysis (ED) cell, several pairs of anion and cation exchange membranes are placed between a pair of planar electrodes, one serving as the anode and the other serving as the cathode. Isolated compartments are formed between each adjacent pair of anion and cation exchange membranes. The electric field imposed by polarization of the cell causes the electromigration of ions, with negatively-charged anions moving through anion exchange membranes towards the positively-charged anode, and positively-charged cations moving through the cation exchange membrane towards the negatively-charged cathode. Ions are forced out of compartments with the same polarity as the cell (even-numbered) and concentrated in compartments having opposite polarity (odd-numbered). Relatively pure water is withdrawn from even-numbered compartments, while the brine phase is recycled to the odd-numbered compartments. Electrolysis causes oxygen evolution at the anode and hydrogen evolution at the cathode. These gaseous reaction products must be continuously removed from the cell. Other electrochemical reactions are also possible, depending upon the impurity ions. Water in the anode compartment becomes acidic due to the accumulation of hydrogen ions, while water in the cathode compartment becomes alkaline due to the accumulation of hydroxyl ions. Elevated pH in the cathode compartment promotes precipitation and accelerates scale formation, and makes rinsing of the electrodes mandatory. Extensive pretreatment of the feedwater is also required to reduce membrane degradation and fouling. Process costs are directly related to the concentration of salt in the feedwater, ie., the amount of current necessary to produce the separation. Electrodialysis reversal (EDR) is a variant of ED with periodic voltage reversal to mitigate scale formation and fouling. In regard to Table 3, it was assumed that EDR requires about 2.0 Wh gal^{-1} (1.9 kJ L^{-1}) per 1000 ppm TDS, with an additional 2.5 Wh gal^{-1} (2.4 kJ L^{-1}) for pumping and an allowance of 5% for instrumentation [3a]. Table 3 indicates that EDR requires 5.8 Wh gal^{-1} (5.5 kJ L^{-1}) to desalinate a 1500 ppm BW stream, and 76.1 Wh gal^{-1} (72.4 kJ L^{-1}) to desalinate SW. Table 4 summarizes the estimated energy requirements for two types of BW desalination plants, RO and EDR, and shows that EDR requires ~7.7 Wh gal^{-1} (7.3 kJ L^{-1}) for desalination of a feed stream with 1600 ppm TDS [4]. Other references indicate that 60-75 Wh gal^{-1} (57-71 kJ L^{-1}) is required by EDR for desalination of SW [5,6].

Flow-Through Capacitors with Activated Carbon Electrodes. There were attempts to desalinate water with activated carbon electrodes in the early 1960's, however, limitations of the electrode materials available at that time prevented further development. The University of Oklahoma appears to have been the first group to use flow-through capacitors with activated carbon electrodes for desalination, with seminal publications that appeared in the early 1960's [7,8]. Activated carbon powders and fibers were held together in electrodes by a variety of polymeric binders. Johnson et al. conducted similar studies of reversible electrosorption with beds of

activated carbon in the early 1970's [9-11]. Johnson's work prompted Newman to develop a comprehensive theoretical model for the capacitive charging of porous carbon electrodes [12]. Additional work was done in Israel several years later and published in the 1980's [13-15]. The work in Israel viewed the process as a chromatographic separation. Several practical problems were encountered with these conventional activated carbon systems. For example, the performance (electrosorption capacity) of activated carbon was found to degrade with time. In electrodes made with polymeric binders, significant fractions of the activated carbon surface was occluded. Electrochemical cells that used flow-through beds of activated carbon powder as electrodes required membrane separators for electrical insulation and to prevent entrainment of individual particles in the flow. Furthermore, flow through such porous media is characterized by high pressure drop. Process efficiency is lowered by large potential drops that develop in thick electrodes, which include packed beds. Finally, early activated-carbon systems had no provisions for the continuous production of pure water, or for the recovery of stored electrical energy. Eventually, this approach to desalination was abandoned.

Capacitive Deionization with Carbon Aerogel Electrodes

Principle of Operation. More recently, an electrochemical process for the capacitive deionization (CDI) of water with stacks of carbon aerogel composite (CAC) electrodes has been developed by Lawrence Livermore National Laboratory [16-24]. An aqueous solution of NaCl, Na_2CO_3, Na_2SO_4 or another salt is passed between numerous pairs of carbon aerogel electrodes, each having a very high BET surface area (2.0-5.4x10^6 ft^2 lb^{-1} or 400-1100 m^2 g^{-1}) and exceptionally low electrically resistivity ($\leq$ 40 mΩ cm). Measured electrosorption capacities, extrapolated to 0.03 N, are on the order of 11.6x10^{-3} lb_{NaCl} lb_C^{-1} (20x10^{-5} equiv g^{-1}). After polarization, ions such as Na^+ and Cl^- are removed from the electrolyte by the imposed electric field and held in electric double layers formed at the surfaces of electrodes. The Gouy-Chapman Theory or the Stern Modification of that theory can be used to describe the effect of an imposed electric field on the surface charge density of the electric double layer [25,26]. As desired, the effluent from the cell is purified water. This process is also capable of simultaneously removing a variety of other impurities. For example, dissolved heavy-metal ions can be removed by reversible electrosorption [27] or by electrodeposition [28-31], in contrast to simple double-layer charging. In the specific case of carbon aerogel CDI, LLNL has investigated a broad range of cell voltages [16-24]. The best performance (salt removal) was achieved at ~1.2-1.3 V, though operation at 0.6 V was found to be possible. Successful testing was done at solution conductivities of 4, 59, 294, 588 and 5,882 ppm (7, 100, 500, 1000 and 10,000 μS cm^{-1}). In routine single-pass experiments, more than 99% of the salt was removed from a 59 ppm (100 μS cm^{-1}) feed stream. After the carbon aerogel electrodes became saturated with salt, breakthrough was observed. Electrodes are regenerated by electrical discharge prior to breakthrough in process applications, which allows the captured salt ions to be released into a relatively small, concentrated purge stream.

Carbon Aerogel Electrodes. Carbon aerogel is an ideal electrode material because of its low electrical resistivity ($\leq$ 40 mΩ cm), high specific surface area (2.0-5.4x10^6 ft^2 lb^{-1} or 400-1100 m^2 g^{-1}), and controllable pore size distribution ($\leq$ 50 nm). Note that thermal and chemical

activation has been used to achieve BET surface areas of $1.3x10^7$ ft^2 lb^{-1} (2600 m^2 g^{-1}) [32]. Resorcinol-formaldehyde (RF) aerogels and their carbonized derivatives were first developed by LLNL [33-36]. Monolithic sheets of this material were made by infiltrating a resorcinol-formaldehyde solution into a porous carbon paper (Textron Specialty Materials, Lowell, MA), curing the wetted paper between glass plates in a closed vessel, and then pyrolizing in an inert atmosphere. The exceptionally high conductivity of this carbon aerogel composite (CAC), in contrast to loosely bonded carbon powders or activated carbon fiber cloths (ACFCs), is attributable to its monolithic structure which is composed of interconnected, covalently-bonded carbon particles, each having a diameter of ~12 nm. In contrast to electrodes made from activated carbon powders and fibers, the activation energy for carrier transport in carbon aerogel is relatively small. These very desirable characteristics have enabled LLNL to use CAC sheets as electrodes in novel supercapacitors with high energy density and high power density [37]. However, these energy-storage devices were not designed to permit electrolyte flow and required membranes to physically separate the electrodes. As discussed here, LLNL has now used CAC electrodes in a variety of configurations to remove ionic contaminants from water. The CAC used to generate the data shown in this publication was produced at LLNL, as well as at GenCorp-Aerojet Plant in Sacramento, California. During this first commercial production campaign, it was demonstrated that a large quantity of high-quality CAC sheets (4000 ft^2 or 372 m^2) could be mass produced at an apparent cost of approximately $50 per square foot. It may be possible to reduce the cost to well below $1-2 per square foot in the future.

Electrochemical Cells. Double-sided electrodes for the electrochemical cell were made by gluing two sheets of the CAC to both sides of a titanium plate with graphite-filled epoxy. The titanium plate served as both a current collector and a structural support. Each sheet of CAC was 4 in x 8 in x 0.010 in (10.16 cm x 20.32 cm x 0.0254 cm) and had a total estimated BET surface area of ~$3.4x10^4$ ft^2 ($3.2x10^7$ cm^2). A typical stack of 150 double-sided, titanium-supported electrodes had a total estimated BET surface area of approximately ~$1.0x10^7$ ft^2 ($9.4x10^9$ cm^2). Electrolyte flowed through the stack in open channels formed between adjacent electrodes. An electrode separation of ~0.027 in (0.069 cm) was maintained in these early cells by rubber compression seals. By arranging the electrodes so that orifices alternate from one side of the stack to the other, flow from the bottom of the stack to the top was serpentine. In desalination applications, the titanium will have to be replaced with a less expensive alternative and smaller electrode separations (gaps) will be required.

Automated Control and Potential-Swing Operation. A prototypical potential-swing system has been developed [24,38]. Ultimately, such synchronous operation will be essential for energy recovery, as well as continuous production, and will require the degree of automation and sophistication that has now been demonstrated. This prototype can produce uninterrupted flows of product and concentrate by operating two stacks of electrodes in parallel. One stack purifies while the other is electrically regenerated. Flow is generated by a programmable, magnetically-coupled, screw pump with a 304 stainless steel head. All lines are made of Teflon and had a nominal diameter of 1/4 in (0.635 cm). The cells are polarized by programmable power supplies that have a voltage range of 0 to 12 V or a current range of 0 to 60 A. Sensors were placed on the inlet and outlet lines of the electrode stack. Electrical conductivity of the solution, pH,

individual ion concentrations, and temperature are continuously monitored. The system is controlled by a personal computer. A single AT-MIO-16DH data acquisition board, installed in the computer, provides the interface to the Input-Output (I/O) Signal Subsystem. The I/O subsystem consists of a single 12-slot Signal Conditioning Extension Interface (SCXI) chassis. The chassis contains seven 8-channel analog-to-digital (A/D) modules to measure flow, level, pressure, temperature, pH, and conductivity; two 16-channel single-pole double-throw (SPDT) relay modules for controlling pumps and valves; and one 6-channel digital-to-analog (D/A) module for controlling power supply voltages and pump speed. The SCXI hardware provides multiplexing, filtering, isolation, and amplification for the process signals. The operating system is DOS v6.22 running Windows v3.1. LabVIEW v3.1 software, running under Windows, is used for data acquisition and control. LabVIEW is a graphical programming environment which provides integrated tools for acquisition, control, analysis, and presentation, as well as connectivity to serial, parallel, voltage, current loop, RTD, thermistor, and relay communication interfaces. Data acquisition and control software is optimized and converted to compiled run-time code. Operator input is via a mouse and keyboard.

Surface Area and Electrosorption Capacity

Interpretation of BET Surface Areas. It is noteworthy that activated carbon powders with Brunauer-Emmet-Teller (BET) surface areas as high as 1.5×10^7 ft^2 lb^{-1} (3000 m^2 g^{-1}) are readily available. However, much of the surface area in such materials is located inside pores having diameters less than 1 nm. It is believed that the electrochemically active area is only a fraction of the BET surface area. BET analyses are probably misleading since gas molecules can penetrate much smaller pores than a typical electrolyte. For example, the bond length of N_2 is only 0.1 nm. It is very doubtful that this level of porosity contributes to electrochemical double layer formation since electrolyte penetration and double layer formation are questionable on this scale. From the Gouy-Chapman theory, as well as the Stern modification of that theory, it is believed that a fully-developed electric double layer on a planar electrode with no detrimental shielding effects would require much greater distances for full development. In the case of a 1:1 electrolyte in water at 25°C, the characteristic thickness of the diffuse layer ranges from 1 nm at a concentration of 0.1 M to 30 nm at 10^{-4} M [26,27]. Though BET surface areas are frequently quoted, the electrosorption capacity, given as equivalents adsorbed per gram of carbon is believed to be a more relevant measure of electrode performance [7,8].

From the Gouy-Chapman theory developed for simple planar electrodes, one might expect the surface charge density to have a square root dependence on electrolyte concentration [25,26]. In the case of dilute aqueous solutions at 25°C, the following expression should be obeyed by both anodes and cathodes:

$$\sigma_{GC} = 11.7\sqrt{C}\,\sinh(19.5\,z\,\phi_0) \qquad [4]$$

where σ_{GC} is the surface charge density (μC cm^{-2}), C is the electrolyte concentration (mol L^{-1}), z is the ionic charge, and ϕ_0 is the electrode potential (mV). However, double layer formation on carbon electrodes is much more complicated. For example, cathode capacities are much higher

than corresponding anode capacities [7,8]. This is attributed to the cation affinity of carbonyl groups on the electrode surface. Therefore, the electrosorption capacity of an electrochemical cell built with porous carbon electrodes is probably limited by its ability to accommodate anions.

Recent data from experiments with NaCl are summarized in Tables 5a and 5b, and illustrated by Figures 1 and 2. Figure 1 shows the electrosorption of Na^+ and Cl^- on 54 double-sided CAC electrodes, each having a width of 4 in and a length of 8 in (10.16 cm x 20.32 cm). The quantity of electrosorbed NaCl (Y) was calculated from the minimum in electrolyte concentration (X_1), reached after polarizing the electrodes for about 55 minutes. The stack of electrodes was maintained at a cell voltage of 1.2 V (X_2) while 0.93 gal (3.5 L) of electrolyte was continuously recycled at a rate of 1.59 gal h^{-1} (X_3, 100 ml min^{-1}). Results for 59, 278 and 588 ppm (100, 500 and 1000 μS cm^{-1}) NaCl solutions are compared. Figure 2 shows electrosorption on 100 double-sided CAC electrodes with the same dimensions as those represented by Figure 1. Approximately 0.79 gal (3 L) of 59 ppm (100 μS cm^{-1}) NaCl solution was continuously recycled at a rate of 1.59 gal h^{-1} (100 ml min^{-1}). Results for 0.6 and 1.2 V are compared. Multiple variable regression analysis of this data was used to determine the dependence of the anion capacity, Y, on equilibium electrolyte concentration, X_1, and cell voltage, X_2. The effects of flow rate were not taken into consideration. The results are summarized by Equation 5:

$$Y = e^{1.3959} X_1^{0.21718} X_2^{2.5883} \qquad [5]$$

where Y has the units of 10^{-5} equivalents per gram of carbon aerogel (based on the anode mass alone), X_1 has the units of 10^{-3} equivalents per liter of solution, and X_2 is given in volts. The agreement between the correlation and experimental data is reasonably good, as illustrated by Figure 3. This is reflected in the calculated multiple-variable regression coefficient, R^2, which is 0.966. A second regression analysis was done, which also accounted for the effects of flow rate, X_3. The results are summarized by Equation 6:

$$Y = e^{2.6730} X_1^{0.27484} X_2^{2.7024} X_3^{-0.27814} \qquad [6]$$

where X_3 is given in ml min^{-1}. Here too the agreement between the correlation and experimental data is good, as illustrated by Figure 4. The calculated multiple-variable regression coefficient, R^2, is 0.942. Since Y and X_1 are directly proportional to σ and C, respectively, one could reasonably expect:

$$Y \propto X_1^{0.5} \qquad [7]$$

It is believed that the failure to observe square-root concentration dependence is due to self-shielding effects experienced by the porous carbon electrodes.

Breakthrough in a Stack of Carbon Aerogel Electrodes

The total area of carbon aerogel sheet required to desalinate a given feed stream (S) can be estimated with the following equation:

$$S \approx \Theta (C_F - C_P) \frac{\tau_B}{\sigma} \qquad [8]$$

where Θ is the volumetric flow rate, C_F is the concentration of salt in the feed stream, C_P is the concentration of salt in the product stream, σ is the area-specific electrosorption capacity of the carbon aerogel at C_F, and τ_B is the breakthrough time. Equation 8 assumes that the concentration shock wave is an abrupt step function. Note that the area-specific electrosorption capacity is:

$$\sigma = FW_{salt}\, \rho_{aerogel}\, \delta_{aerogel}\, Y \qquad [9]$$

where FW_{salt} is the formula weight of the salt, $\rho_{aerogel}$ is the density of the carbon aerogel sheet, $\delta_{aerogel}$ is the thickness of the carbon aerogel sheet, and Y is the electrosorption capacity, calculated with an empirical expression established by linear regression analysis of actual data. As shown in Tables 6a and 7a, the density of CAC sheets was assumed to be 0.413 g cm^{-3} in Cases 1 through 5, and 0.800 g cm^{-3} in Case 6. Then, for example, in Cases 1 through 5:

$$\rho_{aerogel}\, \delta_{aerogel} \approx 0.0105\, g\, cm^{-2} \qquad [10]$$

It should be noted that significant variability in the density of CAC sheets from production campaigns has been observed. Another important time constant is the liquid-phase residence time, τ_R, can be calculated from the channel volume, V, and the volumetric flow rate, Θ.

$$\tau_R \approx \frac{V}{\Theta} \qquad [11]$$

if plug flow is assumed. The liquid volume in the channel is assumed to be:

$$V \approx w L \left(h + 2\theta \delta_{aerogel} \right) \qquad [12]$$

where w is the channel (electrode) width, L is the channel length, h is the electrode separation and θ is the void fraction in the carbon aerogel sheet. Note the relationship between S, L, and w.

$$L = \frac{S}{w} \qquad [13]$$

The void fraction is simply:

$$\theta = 1 - \frac{\rho_{aerogel}}{\rho_{carbon}} \qquad [14]$$

where ρ_{carbon} is assumed to be 2.7 g cm^{-3} (values as low as 2.25 g cm^{-3} can be found in handbooks). Obviously, for the system to work properly, the concentration shock wave must move through the stack more slowly than the liquid:

$$\tau_B \geq \tau_R \qquad [15]$$

The recovery ratio, R, is defined as the fraction of the feed recovered as desalinated product and can be expressed in terms of τ_B and τ_R.

$$R = \frac{\tau_B}{\tau_B + \tau_R} \qquad [16]$$

This assumes that the flow rate during deionization and regeneration are equivalent. In an ideal system, the maximum possible recovery ratio will be about 50% at the point where the two time constants are identical. As τ_B becomes greater than τ_R, the recovery ratio will increase. This criteria can be used to select a consistent electrode separation, which will dictate the pressure drop in the system.

$$h \leq \frac{1-R}{R}\frac{\sigma}{(C_F - C_P)} - 2\delta_{aerogel}(1 - \rho_{aerogel}/\rho_{carbon}) \qquad [17]$$

As the concentration in the feed stream increases, the anode-cathode separation must become smaller. It is important to note combinations of σ and C_F-C_P exist that make it impossible to find a reasonable separation (h would be zero or negative). Alternatively, the minimum possible product concentration can be determined for a fixed electrode separation.

$$C_P \geq C_F - \frac{1-R}{R}\frac{\sigma}{h + 2\delta_{aerogel}(1 - \rho_{aerogel} \cdot \rho_{carbon})} \qquad [18]$$

Clearly, the value of C_p will have to be greater than zero, a requirement that places constraints on C_F, R, σ, h, $\delta_{aerogel}$ and $\rho_{aerogel}$. In Equations 17 and 18, the factor $2\delta_{aerogel}(1-\rho_{aerogel}/\rho_{carbon})$ assumes that the CAC sheets used to construct anodes and cathodes have identical thcknesses. Since the process may be anion limited [8], one might be able to use much thinner CAC sheets for the cathodes than for the anodes, perhaps with $\delta_{cathode} \sim 0.2\delta_{anode}$. In such a case, the factor becomes $1.2\delta_{aerogel}(1-\rho_{aerogel}/\rho_{carbon})$, where $\delta_{aerogel}$ is the thickness of the CAC sheets used to make the anodes. By using the thinnest possible cathode, larger electrode gaps can be tolerated and lower product concentrations can be achieved.

Minimum Energy Required for Separation

The minimum work of separation of a feed mixture into impure products at constant temperature and pressure can be computed with Equation 19 [39]:

$$W_{\min,T} = -RT\left(\sum_j x_{jF}\ln(\gamma_{jF}x_{jF}) - \sum_i \phi_i \sum_j x_{ji}\ln(\gamma_{ji}x_{ji})\right) \qquad [19]$$

where ϕ_i is the molar fraction of feed entering product i, x_{ji} is the mole fraction of component j in product i, and γ_{ji} is the activity coefficient of component j in product i. For a binary mixture, Equation 19 becomes:

$$W_{\min,T} = -\frac{RT}{x_{A1}-x_{A2}}\left\{\begin{array}{l}(x_{AF}-x_{A2})\left[x_{A1}\ln\dfrac{\gamma_{AF}x_{AF}}{\gamma_{A1}x_{A1}} + (1-x_{A1})\ln\dfrac{1-x_{AF}}{1-x_{A1}}\right] \\ +(x_{A1}-x_{AF})\left[x_{A2}\ln\dfrac{\gamma_{AF}x_{AF}}{\gamma_{A2}x_{A2}} + (1-x_{A2})\ln\dfrac{1-x_{AF}}{1-x_{A2}}\right]\end{array}\right\} \qquad [20]$$

The Debye-Huckel model [40] can be used to estimate the activity coefficient of component j:

$$\ln\gamma_j = -\frac{z_j^2\alpha'\sqrt{I'}}{1+B'a\sqrt{I'}} \qquad [21]$$

where a is the exclusion distance of a central ion located at the origin, z_j is the valence of species j, I' is the molar ionic strength, and α' and B' are the Debye-Huckel parameters. The molar ionic strength is:

$$I' = \frac{1}{2}\sum_j z_j^2 c_j \qquad [22]$$

where c_j is the molar concentration of species j. The Debye Huckel parameters are defined as:

$$B' = \frac{F}{\sqrt{\varepsilon RT/2}} \qquad [23]$$

$$\alpha' = \frac{Fe}{8\pi\varepsilon RT}B \qquad [24]$$

where R is the universal gas constant, T is the absolute temperature, F is Faraday's constant, e is the electronic charge, and ε is the permittivity. As the ionic strength goes to zero, the Debye-Huckel limiting law becomes:

$$\ln\gamma_j \approx -z_j^2\alpha'\sqrt{I'} \qquad [25]$$

Equations 20 through 25 were used to calculate the minimum energy requirements for desalination as a function of NaCl concentration. Results are summarized in Tables 6e, 6f and 7f. The minimum energy required for separation of a 2000 ppm NaCl stream into a 100 ppm product and a concentrate with R=0.5 is ~0.095 Wh gal^{-1} (0.090 kJ L^{-1}), whereas the minimum energy required for separation of a 35,000 ppm NaCl solution (surrogate SW) into a 100 ppm product and a concentrate with R=0.5 is ~2.0 Wh gal^{-1} (1.9 kJ L^{-1}).

Electrical Energy Requirement

The energy stored in the electrochemical cell during charging (deionization) can be estimated from the expression for an ideal capacitor:

$$U_{stored} = \frac{1}{2} QV \qquad [26]$$

where Q is the stored electrical charge and V is the cell voltage. Stored energy is available for recovery during discharge (regeneration). Equation 16 accounts for the energy consumed by parasitic electrochemical reactions:

$$U_{parasitic} = V \int_0^t I_p(t)\,dt \qquad [27]$$

where $I_p(t)$ is the instantaneous current due to parasitic charge-transfer reactions and t is the time required for deionization. Ohmic losses must also be accounted for:

$$U_{ohmic} = \int_0^t R(t)\left[I_c(t) + I_p(t)\right]^2 dt \qquad [28]$$

where $I_c(t)$ is the instantaneous current due to deionization and $R(t)$ is the instantaneous electrical resistance. The ohmic loss associated with the parasitic current is implicit in Equation 27, and is included explicitly in Equation 28. Consequently, when these two contributions are summed to calculate the total energy consumption, the estimate will be slightly higher than the actual value (conservative). Note that $I_p(t)$, $I_c(t)$ and $R(t)$ are spatially-averaged quantities, representing the entire stack of electrodes. At this point, a reasonable approximation for an order-of-magnitude esimate can be derived by treating the currents and the resistance as a time-average quantities.

$$U_{parasitic} \approx V\, I_p\, \Delta t \qquad [29]$$

$$U_{ohmic} \approx R\left\{\left(\frac{Q}{\Delta t}\right) + I_p\right\}^2 \Delta t \qquad [30]$$

The energies per unit volume of product, W_{stored}, $W_{parasitic}$, and W_{ohmic}, are calculated by dividing U_{stored}, $U_{parasitic}$ and U_{ohmic}, respectively, by the volume of water processed per unit time:

$$W_{stored} = \frac{U_{stored}}{\Theta \Delta t} \quad [31]$$

$$W_{parasitic} = \frac{U_{parasitic}}{\Theta \Delta t} \quad [32]$$

$$W_{ohmic} = \frac{U_{ohmic}}{\Theta \Delta t} \quad [33]$$

where Θ is the volumetric flow rate of product during the interval Δt.

Parasitic Current: Limited by Diffusion and Fixed Reactant Mass

The observed parasitic current may be due to a fixed mass of electroactive reactant introduced with the feed. One possibility might be the reduction of dissolved oxygen:

$$O_2 + 2H_2O + 4e^- \xrightarrow{electrode} 4OH^- \quad [34]$$

which has a standard reduction potential of 0.401 V measured against a standard hydrogen electrode (SHE). The depletion of such a reactant is assumed to be limited by mass transport to the electrode-electrolyte interface. For simplicity, we assume that this interface is the outer surface of the monolithic sheet of carbon aerogel. The diffusive flux of such non-ionic species to the surface of the electrode is:

$$J = -D\frac{\partial C}{\partial y} \approx -D\frac{\Delta C}{\Delta y} \approx k\Delta C \quad [35]$$

where D is the diffusivity (~10^{-5} cm^2 s^{-1}), C is reactant concentration in the bulk electrolyte (mol cm^{-3}), k is the mass transfer coefficient (cm s^{-1}), and y is the direction normal to the carbon aerogel electrode. The maximum possible flux coincides with a zero surface concentration ($\Delta C = C$). Note that the mass transfer coefficient can be calculated from a dimensionless correlation such as the Sherwood equation:

$$\frac{k D_e}{D} = 0.023\left(\frac{D_e u_b \rho}{g_c \mu}\right)^{0.8}\left(\frac{\mu}{\rho D}\right)^{0.33} \quad [36]$$

The term on the LHS of the equation is known as the Sherwood number (Sh), the first term on the RHS is known as the Reynolds number (Re), and the second term on the RHS is the Schmidt number (Sc). A mass balance on a differential length of the electrochemical cell channel yields:

$$\frac{dC}{dx} = -\frac{w}{\Theta} k C \qquad [37]$$

where Θ is the volumetric flow rate. Integration of this expression yields the reactant concentration as a function of channel length.

$$C = C_F \exp\left[-\frac{wkx}{\Theta}\right] \qquad [38]$$

where C_F is the concentration of the reactant in the feed, w is the electrode (channel) width, and x is the channel length. The current density is then defined in terms of this diffusive flux:

$$i = nFJ \approx nFk\Delta C \qquad [39]$$

where n is the number of electrons involved in the electrochemical reaction and F is Faradays constant. The limiting current is calculated from the maximum possible flux, the point where the surface concentration is zero ($\Delta C = C$).

$$i_L = nFJ_{\max} \approx nFkC \qquad [40]$$

Note that this quantity is a function of position along the channel.

$$i_L(x) = nFkC_F \exp\left[-\frac{wkx}{\Theta}\right] \qquad [41]$$

The total parasitic current due to this diffusion-limited electrochemical reaction is calculated with the following integral:

$$I_p = w\int_o^L i_L(x)\,dx \qquad [42]$$

The integration yields:

$$I_p = n\,F\,C_F\,\Theta\left(1-\exp\left[-\frac{wkx}{\Theta}\right]\right) \qquad [43]$$

This can be used as the basis of scaling a measured parasitic current to any channel length:

$$\frac{I_{P,x_1}}{I_{P,x_2}} = \frac{1-\exp\left[-\frac{wkx_1}{\Theta}\right]}{1-\exp\left[-\frac{wkx_2}{\Theta}\right]} \qquad [44]$$

The parasitic current can be expressed in terms of the total number of stacks, N.

$$I_{P,N} = I_{P,N=1}\frac{1-\exp\left[-\frac{wk\Delta x\, N}{\Theta}\right]}{1-\exp\left[-\frac{wk\Delta x}{\Theta}\right]} \qquad [45]$$

where Δx is the channel length of a single stack. The maximum possible value of I_p is found by taking the limit as N approaches infinity.

$$\lim_{N\to\infty} I_{P,N} = I_{P,N=1}\frac{1}{1-\exp\left[-\frac{wk\Delta x}{\Theta}\right]} \qquad [46]$$

An order-of-magnitude estimate of the parasitic current as a function of total channel length or the number of stacks can be made. For example, assume that $h \geq 0.069$ cm $\geq d$, $w \sim 10.16$ cm, Δx ~ 3000 cm, $D \sim 10^{-5}$ cm^2 s^{-1} and $\Theta \sim 100$ cm^3 min^{-1}. In this case, the parasitic current for an infinite number of stacks is only 5% greater than the parasitic current for a single stack. In this case, there is no energy penalty for increasing the channel length.

Parasitic Current: In Situ Generation of Reactants Governed by Cell Voltage

The observed parasitic current might also be due to very low levels of electrolysis at both electrodes. In this scenario, oxygen generated at the anode would dissolve in the water. After being tranported to the cathode, it would undergo reduction. Hydroxyl ions produced at the cathode during oxygen reduction would then be transported to the anode, where oxidation would provide additional oxygen. Thus, a continuous cycle would be established and no decline in the parasitic current density over the length of the channel would be observed. In such a case, it could be assumed that the parasitic current density, i (μA cm^{-2}), would obey the following empirical expression:

$$\ln(i) = A + B\Delta V \qquad [47]$$

where A and B are temperature-dependent empirical constants, and ΔV (V) is the cell voltage. Some preliminary data suggests that:

$$\ln(i) = 1.221 + 1.5069\Delta V \qquad [48]$$

Based on this empirical equation, the parasitic current density would be expected to be about 18.7 μA cm^{-2} at 1.2 V, and 7.6 μA cm^{-2} at 0.6 V.

Mechanical Energy Requirement

The mechanical energy balance for an incompressible fluid is given as Equation 49 [41-43]:

$$\frac{\Delta u_b^2}{2g_c} + \frac{g}{g_c}\Delta z + \frac{\Delta p}{\rho} + lw_f + \eta_{pump} W_{pump} = 0 \qquad [49]$$

where u_b is the change in average velocity of the electrolyte in the open channel between pairs of CAC electrodes, g is the gravitational acceleration, g_c is the gravitational constant, z is the elevation, p is the pressure, ρ is the electrolyte density, lw_f is the lost work due to friction, η_{pump} is the efficiency of the pump, and W_{pump} is the energy required by the pump. The lost work due to friction, based upon the Fanning friction factor, is:

$$lw_f = \frac{2f^* L u_b^2}{g_c D_e} \qquad [50]$$

where D_e is the equivalent diameter, defined as four times (4X) the hydraulic radius, r_h. The hydraulic radius is defined as the cross-sectional area of the channel divided by the wetted perimeter:

$$r_h = \frac{w \times h}{2(w+h)} \qquad [51]$$

The electrode width and separation are w and h, respectively. The Fanning friction factor is then defined as:

$$f^* = \frac{g_c D_e (-\Delta p)}{2 u_b^2 \rho L} \qquad [52]$$

Alternatively, the lost work due to friction, based upon the Moody friction factor, is:

$$lw_f = \frac{f L u_b^2}{2 g_c D_e} \qquad [53]$$

The Moody friction factor is defined as:

$$f = \frac{2 g_c D_e (-\Delta p)}{u_b^2 \rho L} \qquad [54]$$

Early work done with pipes indicates that [41]:

$$f = \frac{64}{\mathrm{Re}} \qquad [55]$$

The Reynolds number is defined as:

$$\mathrm{Re} = \frac{D_e u_b \rho}{g_c \mu} \qquad [56]$$

where μ is the viscosity. A regression analysis of experimental pressure-drop data indicates that the Moody friction factor for a stack of 150 double-sided carbon aerogel electrodes is:

$$f = \frac{14.3766}{\mathrm{Re}^{0.72917}} \qquad [57]$$

The y variance was 0.206, the x-y variance was 0.011, and the regression coefficient was 0.953, all indicating a good fit to the data. The regression equation is compared to the actual data in Figure 5. The difference between Equations 55 and 57 is probably due to slippage of fluid at the boundary between the aerogel and the open channel where the water is assumed to flow. More slippage would be expected at a fluid-filled porous wall than at a solid wall, and would lower the effective friction factor. Note that the sheets of carbon aerogel were 4 in x 8 in x 0.010 in (10.2 cm x 20.3 cm x 0.025 cm); the epoxy film used to glue the carbon aerogel to the titanium substrate was approximately 0.0025 in (0.0064 cm) thick; and the gaskets used to separate the titanium plates were 0.062 in (0.16 cm) thick without compression and about 0.052 in (0.13 cm) thick with compression. The gap separating adjacent sheets of carbon aerogel were approximately 0.027 in (0.069 cm). The corresponding hydraulic radius was 0.0134 in (0.0341 cm) and the equivalent diameter was 0.0536 in (0.136 cm). The energy requirement for pumping is approximately 7.2×10^{-3} Wh gal^{-1} psi^{-1}.

Total Energy Requirement

The total energy requirement per unit volume of product is then calculated as:

$$W_{total} = (1-\varepsilon) W_{stored} + W_{parasitic} + W_{ohmic} + \frac{1}{R} W_{pump} \qquad [58]$$

where ε is the fraction of the stored electrical energy that is recovered during discharge, or regeneration of the stack. The other terms are defined by Equations 16, 31, 32, 33 and 49, respectively. An energy recovery of approximately 50% ($\varepsilon \sim 0.5$) should be relatively easy to achieve since no voltage conversion should be required. With voltage conversion, approximately 70% ($\varepsilon \sim 0.7$) should be possible. As already discussed in regard to Equations 27 and 28, the ohmic loss associated with the parasitic current are accounted for twice, which leads to a

conservative estimate. However, the result is inconsequental since the ohmic losses are relatively insignificant.

Results of Energy Analysis

Theoretical Minimum. As previously discussed, the minimum theoretical work required by an isothermal process to separate SW or BW into product and concentrate streams can be calculated with equations 19 through 25. If SW and BW are assumed to be NaCl solutions, Equation 20 can be used (as was done here). This calculation requires that the activity coefficient of NaCl be estimated with the Debye-Huckel Theory. Assuming a recovery ratio of 0.5, the theoretical minimum work for separation of SW (35,000 ppm NaCl) or BW (2000 ppm NaCl) into product (100 ppm NaCl) and concentrate streams are ~2.0 Wh gal^{-1} (1.9 kJ L^{-1}) or ~0.10 Wh gal^{-1} (0.09 kJ L^{-1}), respectively. All estimates of the required energy for carbon aerogel CDI under these conditions should be greater than these limiting values.

Estimated Energy Requirements for Carbon Aerogel CDI. Cases 1 through 6 in Tables 6a through 6f, which are illustrated by Figures 6a through 6f, are scenarios where the minimum possible product concentration was fixed at 100 ppm, the recovery ratio was fixed at 0.5 (except Case 6), and the maximum possible electrode gap was calculated. Case 6 assumed a recovery ratio of 0.85. Cases 1 through 6 in Tables 7a through 7i, illustrated by Figures 7a through 7f, are scenarios where the electrode gap was fixed, which enabled calculation of the maximum possible recovery ratio, R, and the minimum possible product concentration, C_p. The "Energy Requirement - No Depletion" assumes that the electroactive species responsible for the parasitic current is generated in situ and not depleted, whereas the "Energy Requirement - With Depletion" assumes that the electroactive species is introduced in the feed (dissolved oxygen, etc.) and is depleted by the parasitic electrode reaction. By treating the channel like a plug-flow reactor, depletion factors can be calculated (Equations 37 through 46]. Note that some reasonably attractive cases for brackish water were identified, but no good combination of parameters for sea water was found. In particular, Cases 3 and 6 in Tables 7a through 7i appear to have relatively low energy requirements, as well as reasonable recovery ratios. As specified in Case 6, it will be necessary to use thicker, more dense CAC sheets ($\delta_{aerogel}$ ~ 0.127 cm, $\rho_{aerogel}$ ~ 0.8 g cm^{-3}) than currently available in prototypes to achieve high recovery ratios (R ~ 0.863-0.890). Such a system, with an electrode separation of about 13.8×10^{-3} in (0.035 cm), should be able to desalinate BW (1500-2000 ppm) with an energy requirement of ~0.53-1.06 Wh gal^{-1} (0.50-1.01 kJ L^{-1}). This case is compared to RO and EDR in Table 8.

Comparison of Competing Technologies for Desalination. Competiting technologies for SW desalination include reverse osmosis (RO), mechanical vapor recompression (MVC), electrodialysis (ED), multistage flash (MSF), multiple effect distillation with mechanical vapor recompression (MED-MVC) and multiple effect distillation with thermal vapor recompression (MED-TVC). Published data indicates that RO consumes ~25-36 Wh gal^{-1} (24-34 kJ L^{-1}), MVC consumes ~30-41 Wh gal^{-1} (29-39 kJ L^{-1}), ED consumes ~60-75 Wh gal^{-1} (57-71 kJ L^{-1}), MED-TVC consumes ~215-315 Wh gal^{-1} (205-300 kJ L^{-1}), MSF consumes ~320 Wh gal^{-1} (304 kJ L^{-1}), and simple evaporation without energy recovery consumes ~2720 Wh gal^{-1} (2586 kJ L^{-1}). In the case of RO, lower energy requirements can be achieved through the use of energy recovery

turbines. The intrinsic energy requirement for SW desalination with carbon aerogel CDI is *QV/2*, which is ~36-37 Wh gal^{-1} (34-35 kJ L^{-1}). An energy requirement less than that needed for RO can be envisioned through the use of potential-swing operation with energy recovery; however, practical constraints on cell geometry, aerogel properties and product concentration make this specific application of carbon aerogel CDI very challenging. The primary competing technologies for BW desalination are electrodialysis reversal (EDR) and reverse osmosis (RO). Published estimates for the desalination of 1600 ppm BW indicates that RO consumes ~8.5 Wh gal^{-1} (8.1 kJ L^{-1}), while ED consumes ~7.7 Wh gal^{-1} (7.3 kJ L^{-1}). The estimated energy requirement for desalination of 2000 ppm BW with carbon aerogel CDI is ~0.53-2.5 Wh gal^{-1} (0.50-2.4 kJ L^{-1}), depending upon voltage, flow rate, energy recovery, electrode gap, CAC density and thickness, and other important variables. As previously discussed, the estimated energy requirements for BW desalination with carbon aerogel CDI, RO and EDR are compared in Table 8.

Discussion

Parasitic Current. From the analysis presented in Tables 6a through 7i, it is evident that the open-channel cell design used in carbon aerogel CDI minimizes the mechanical energy required for pumping to a level where energy requirements are dominated by the stored electrical energy and the energy consumed by parasitic electrochemical reactions such as oxygen reduction. Note that the cell design also minimizes ohmic losses to a very low level. Clearly, efforts to improve process efficiency should be directed towards the elimination or avoidance of parasitic cell current. It is believed that this can be done through stripping, catalytic surfaces that eliminate reactants upstream, the use of suitable electrode poisons (inhibitors), or other conductive aerogels with greater activation overpotentials for oxygen reduction and other relevant reactions. Additional work needs to be done to quantitatively determine parasitic current as a function of all relevant operating parameters.

Relative Challenges of BW and SW Applications. SW applications will require much larger quantities of aerogel for the electrosorption of salt than BW applications. In this respect, SW applications are expected to be more difficult. However, SW applications are more tolerant of low recovery (product/feed) ratios, which could be advantageous. Recovery ratios of 0.50-0.85 are required for BW desalination, whereas values as low as 0.15 have been found acceptable for some SW desalination processes.

Scale Formation. Most of the salts found in SW and BW have inverted solubilities, which means that their solubilities decrease with increasing temperature. Thus, precipitation and scale-formation problems encountered at heat transfer surfaces in thermal desalination processes such as MED-TVC, MED-MVC and MSF become worse as operating temperatures are increased. Furthermore, the thermal decomposition of carbonates such as $CaCO_3$ produces CO_2 and scale-forming hydroxides. Such scale formation can be mitigated by suppressing the pH with HCl or H_2SO_4 additions to the feed. Unfortunately, such acid dosing accelerates corrosion and can contribute to scale formation through the formation of $CaSO_4$, which is also relatively insoluble. By using ion exchange columns to remove scale-forming solutes such as Ca^{2+} and Mg^{2+}

(hardness) from SW and BW, a relativley soft NaCl solution is obtained. This softened stream can then be fed to the evaporator of a thermal desalination process with substantially less risk of scale formation. This strategy has been explored by Donath [44]. RO, ED and EDR are also susceptible to scale-formation. As previously discussed, concentration polarization at the brine-membrane interface in a RO system can result in localized supersaturation, precipitation and scale formation. Here too chemicals are added to the feed to help minimize scale formation problems. The ion separation inherent in carbon aerogel CDI results in the formation of high-solubility acids and bases at anodes and cathodes, respectively, during regeneration (discharge). Thus, scale formation due to precipitation from supersaturated solution at the electrode-electrolyte interface is avoided.

Other Operational Advantages of Carbon Aerogel CDI. Compressor maintenance and repair required by MVC and MED-MVC are avoided. Since no membranes or high pressure pumps are needed, carbon aerogel CDI also offers operational advantages over RO, ED and EDR. Standard pressure RO systems require differential pressures of 400-650 psi (27-44 atm), while low-pressure systems require 200-300 psi (14-20 atm). The pressure drop across a carbon aerogel CDI system used for BW desalination is expected to be far less (Tables 6a & 6d; 7a & 7e). Typically, the shelf life of RO membranes is 3 to 5 years, requiring cold storage during that period of time. Carbon aerogel electrodes have an indefinite shelf life and require no cold storage. Furthermore, RO membranes are susceptible to many of the chemicals used for water treatment. Note that polyamide has been found to be sensitive to attack by chlorine, whereas carbon aerogel is believed to be relatively resistant. The cost of replacing damaged membranes is significant. Membrane replacement accounted for ~52% of the production cost in early RO systems [43], and for ~32% in more recent systems [4]. In modern RO plants, membrane replacement is believed to account for ~15% of the production cost. These costs will be driven to higher values if more expensive membranes are used.

Recent Improvements in RO Technology. Recent improvements in RO technology may lead to improved energy efficiency [47]. The cost of desalinating 1000 gallons of oceanic SW (~35,000 ppm) with RO is given as $3.34 by Shield and Moch. In their computational analysis, approximately 40% of that cost appears to be due to the required electrical power. Since they assume that electrical power costs approximately $0.08 per kW, the corresponding electrical power requirement must have been 17-18 Wh gal^{-1} (16-17 kJ L^{-1}). No estimates for BW desalination are given. Carbon aerogel CDI could be used as a polishing process for low-concentration product streams from such high-efficiency processes.

Selective Removal of Ions. Ion exchange is now used to remove heavy metals from contaminated ground water. Unfortunately, the chemical regeneration of saturated ion exchange resin produces a significant amount of secondary waste. A variety of electrochemical alternatives to ion exchange are now under investigation. For example, polypyrolle films on reticulated vitreous carbon electrodes are being used for in situ reduction of Cr(VI) [45]. This approach appears to suffer from a gradual degradation of the electrodes due to a loss of polypyrolle. Another process involves the use of electrodes coated with films of electroactive ferrocyanide for selective removal Cs^+ from solutions of sodium salts [46]. Here too electrode life may be limited by the

stability of the electroactive film. Carbon aerogel electrodes appear to have the necessary selectivity and stability to enable them to serve as a viable alternative to ion exchange. Treatability tests at LLNL have shown that 35 ppm Cr(VI) can be selectively removed from contaminated ground water with a 530 ppm TDS background [24,27]. Reversibility was demonstrated by quantitiative recovery of all electrosorbed chromium during regeneration. Carbon aerogel CDI has also been used to remove Cu, Zn, Cd, Pb, Cr, Mn, Co and U from process solutions and natural waters by electrosorption on CAC electrodes [24]. This type of application was the incentive for development of carbon aerogel CDI.

Summary

The minimum theoretical work required by an isothermal process to separate sea water (~35,000 ppm NaCl) or brackish water (~1000-10,000 ppm NaCl) into product and concentrate streams has been calculated. This calculation requires that the activity coefficient of NaCl be estimated with the Debye-Huckel Theory. Assuming a recovery ratio of 0.5, the minimum theoretical work required for separation of SW (35,000 ppm NaCl) into product (100 ppm NaCl) and concentrate streams is ~2.0 Wh gal^{-1} (1.9 kJ L^{-1}), whereas the minimum theoretical work for generating the same product from BW (2000 ppm NaCl) is only ~0.10 Wh gal^{-1} (0.09 kJ L^{-1}). Data from several operating desalination processes were published by Wade in 1993 [2]. His work indicates that RO consumes ~25-36 Wh gal^{-1} (24-34 kJ L^{-1}), MVC consumes ~30-41 Wh gal^{-1} (29-39 kJ L^{-1}), ED consumes ~60-75 Wh gal^{-1} (57-71 kJ L^{-1}), MED-TVC consumes ~215-315 Wh gal^{-1} (205-300 kJ L^{-1}), and MSF consumes ~320 Wh gal^{-1} (304 kJ L^{-1}). Simple evaporation without energy recovery consumes ~2720 Wh gal^{-1} (2587 kJ L^{-1}). More recent computational analysis by Shields and Moch assumes that RO requires 17-18 Wh gal^{-1} (16-17 kJ L^{-1}) [47]. The intrinsic energy requirement for SW desalination with carbon aerogel CDI is $QV/2$, which is ~36-37 Wh gal^{-1} (34-35 kJ L^{-1}). An energy requirement less than that needed for RO can be envisioned through the use of potential-swing operation with energy recovery; however, practical constraints on cell geometry, aerogel properties and product concentration make this specific application of carbon aerogel CDI very challenging. The primary competing technologies for BW desalination are electrodialysis reversal (EDR) and reverse osmosis (RO) [3a,3b,4]. Published data for the desalination of 1600 ppm BW indicates that RO consumes ~8.5 Wh gal^{-1} (8.1 kJ L^{-1}), while ED consumes ~7.7 Wh gal^{-1} (7.3 kJ L^{-1}). The estimated energy requirement for desalination of 2000 ppm BW with carbon aerogel CDI is ~0.53-2.5 Wh gal^{-1} (0.50-2.4 kJ L^{-1}), depending upon voltage, flow rate, energy recovery, electrode gap, CAC density and thickness, and other important variables. Attractive scenarios for BW desalination have been found; however, cell designs have demanding tolerances. With additional investments in research and development, it may be possible to develop carbon aerogel CDI to a point where practical, large-scale desalination of BW is possible. However, such applications will probably require significant reductions in the costs of the aerogel materials.

Carbon aerogel electrodes have demonstrated the necessary selectivity and stability to enable them to serve as a viable alternative to ion exchange resins for the remediation of Cr(VI)-contaminated ground water. Field tests at LLNL have shown that carbon aerogel electrodes can be used to selectively remove 35 ppb Cr(VI) from contaminated ground water with a 530 ppm

TDS background. Consequently, it may be possible to avoid the generation of large quantities of secondary waste, produced during chemical regeneration of ion exchange columns.

Future Work

Since numerous assumptions were made to render computations tractable, the estimates presented here are imperfect. As knowledge of this novel aerogel-based process improves, calculations should be refined. Furthermore, experimental data from experiments with concentrated NaCl and actual BW should be used to verify predictions.

Estimation of the minimum product concentration, C_P, should be improved. These calculations evaluate the area-specific electrosorption capacity, σ, at the feed concentration, C_F. Since the electrodes become saturated with salt at the point when equilibrium is established between the feed stream and the carbon aerogel, this seems like a reasonable assumption. However, immediately following polarization, the equilibrium established at the stack outlet is at C_f instead of C_F. In the future, any equation used to estimate the minimum product concentration should use a value of σ evaluated at the outlet conditions.

Ultimately, the concentration profile in the stack of carbon aerogel electrodes should be calculated by analytically or numerically integrating the first-order hyperbolic partical differential equations that describe the system. The analytical methods for chromatographic systems outlined by Rhee, Aris and Amundsen are believed to be applicable [48]. Chiba has solved the equations for a carbon aerogel CDI system numerically [49]. Both sources should be consulted.

To overcome limitations in product concentration, parametric pumping should be explored. For example, feed should be admitted after polarization so that a steep concentration gradient can be established along the length of the channel (stratification of the column). Subsequently, the electrodes should be electrically discharged (regenerated) with zero flow (stagnant). After discharge, the concentrate should be removed from the high-concentration end of the stack, where the feed is introduced. Such reverse flow (backflushing) should enable the steep concentration gradient to be maintained. Gas displacement may be required. Some aspects of this mode of operation have already been explored by Oren and Soffer [13-15].

Acknowledgment

Contributions of R. W. Pekala are gratefully acknowledged. Funding for initial process development was provided by the Strategic Environmental Research and Development Program (SERDP). Funding and the opportunity to explore desalination applications has been provided by the Alameda County Water District in California. This work was done under the auspices of the U.S. Department of Energy (DOE) by Lawrence Livermore National Laboratory (LLNL) under Contract No. W-7405-Eng-48.

References

1. L. J. Summers, "Desalination Processes and Performance," Lawrence Livermore National Laboratory, UCRL-ID-120367, June 14 (1995).

2. N. M. Wade, "Technical and Economic Evaluation of Distillation and Reverse Osmosis Desalination Processes," Desalination, Vol. 93, pp. 343-363, (1993).

3a. W. J. Conlon, "Membrane Processes," Chapt. 11, Water Quality and Treatment, A Handbook of Community Water Supplies, 4th Ed., R. W. Pontius, Ed., American Water Works Association, McGraw-Hill, San Francisco, CA, pp. 709-746 (1990).

3b. R. M. Clark, "Water Supply," Chapt. 5, Standard Handbook of Environmental Engineering, R. A. Corbitt, Ed., McGraw-Hill, San Francisco, CA, pp. 5.146-149 (1989).

4. R. C. Harries, D. Elyanow, "Desalination of Brackish Groundwater for a Prarie Community Using Electrodialysis Reversal," Desalination, Vol. 84, pp. 109-121, (1991).

5. A. H. Khan, Desalination Processes and Multistage Flash Distillation Practice, Desalination and Water Purification, Vol. 1, Elsevier, New York, NY, pp. 124-137, 162-168, 570-586 (1986).

6. P. K. Narayanan, S. K. Thampy, N. J. Dave, D. K. Chauhan, B. S. Makwana, S. K. Adhikary, V. K. Indusekhar, "Performance of the First Sea Water Electrodialysis Desalination Plant in India," Desalination, Vol. 84, pp. 201-211, (1991).

7. B. B. Arnold, G. W. Murphy, "Studies on the Electrochemistry of Carbon and Chemically Modified Carbon Surfaces," J. Phys. Chem., Vol. 65, No. 1, pp. 135-138 (1961).

8. D. D. Caudle, J. H. Tucker, J. L. Cooper, B. B. Arnold, A. Papastamataki, "Electrochemical Demineralization of Water with Carbon Electrodes," Research and Development Progress Report No. 188, United States Department of Interior, 190 pages, May (1966).

9. A. M. Johnson, A. W. Venolia, J. Newman, R. G. Wilbourne, C. M. Wong, , W. S. Gillam, S. Johnson, R. H. Horowitz, "Electrosorb Process for Desalting Water," Office of Saline Water Research and Development Progress Report No. 516, U.S. Dept. Interior Pub. 200 056, 31 pages, March (1970).

10. A. M. Johnson, A. W. Venolia, R. G. Wilbourne, J. Newman, "The Electrosorb Process for Desalting Water," Marquardt Co., Van Nuys, CA, 36 pages, March (1970).

11. A. M. Johnson, "Electric Demineralizing Apparatus," U.S. Pat. No. 3515664, June 2 (1970).

12. A. M. Johnson, J. Newman, "Desalting by Means of Porous Carbon Electrodes," J. Electrochem. Soc., Vol. 118, No. 3, pp. 510-517 (1971).

13. Y. Oren, A. Soffer, "Electrochemical Parametric Pumping," J. Electrochem. Soc., Vol. 125, No. 6, pp. 869-875 (1978).

14. Y. Oren, A. Soffer, "Water Desalting by Means of Electrochemical Parametric Pumping: I. The Equilibrium Properties of a Batch Unit Cell," J. Appl. Electrochem., Vol. 13, No. 4, pp. 473-487 (1983).

15. Y. Oren, A. Soffer, "Water Desalting by Means of Electrochemical Parametric Pumping: II. Separation Properties of a Multistage Column," J. Appl. Electrochem., Vol. 13, No. 4, pp. 489-505 (1983).

16. J. C. Farmer, "Method and Apparatus for Capacitive Deionization, Electrochemical Purification, and Regeneration of Electrodes," U.S. Pat. No. 5428858, June 20 (1995).

17. J. C. Farmer, D. V. Fix, G. V. Mack, R. W. Pekala, J. F. Poco, "The Use of Capacitive Deionization with Carbon Aerogel Electrodes to Remove Inorganic Contaminants from Water," Proc. 1995 Intl. Low-Level Conf., Orlando, Florida, July 10-12, 1995, Electric Power Research Institute, Palo Alto, CA, Rept. TR-105569, pp. 42 1-23 (1995).

18. J. C. Farmer, D. V. Fix, G. V. Mack, R. W. Pekala, J. F. Poco, "Capacitive Deionization of Water: An Innovative New Process," Proc. Fifth Intl. Conf. Rad. Waste Mgmt. Environ. Remediation, Berlin, Germany, September 3-9, 1995, American Society of Mechanical Engineers (ASME), New York, NY, Vol. 2, pp. 1215-1220 (1995).

19. J. C. Farmer, D. V. Fix, G. V. Mack, R. W. Pekala, J. F. Poco, "Capacitive Deionization with Carbon Aerogel Electrodes: Carbonate, Sulfate, and Phosphate," Proc. 1995 Intl. SAMPE Tech. Conf., Albuquerque, NM, October 9-12, 1995, Society for the Advancement of Material and Process Engineering (SAMPE), Covina, CA, Vol. 27, pp. 294-304 (1995).

20. J. C. Farmer, D. V. Fix, G. V. Mack, R. W. Pekala, J. F. Poco, "Capacitive Deionization of NaCl and $NaNO_3$ Solutions with Carbon Aerogel Electrodes," J. Electrochem. Soc., Vol. 143, No. 1, pp. 159-169 (1996).

21. J. C. Farmer, D. V. Fix, G. V. Mack, R. W. Pekala, J. F. Poco, "Capacitive Deionization of NH_4ClO_4 Solutions with Carbon Aerogel Electrodes," J. Appl. Electrochem., Vol. 26 (Ms. No. NA-025-95, in press) (1996).

22. J. C. Farmer, D. V. Fix, R. W. Pekala, J. K. Nielsen, A. M. Volpe, D. D. Dietrich, "The Use of Carbon Aerogel Electrodes for Environmental Cleanup," Proc. Symposium on the Production and Use of Carbon-Based Materials for Environental Cleanup, 1996 Spring Meeting of the American Chemical Society, New Orleans, Louisiana, March 24-29, 1996. Vol. 41, p. 484 (1996).

23. J. C. Farmer, R. W. Pekala, F. T. Wang, D. V. Fix, A. M. Volpe, D. D. Dietrich, W. H. Siegel, "Electrochemical and Photochemical Treatment of Aqueous Waste Streams," Proc. Spectrum 96, Nucl. Haz. Waste Mgmt. Intl. Topical, , Seattle, Washington, August 18-23, 1996, Am. Nucl. Soc., La Grange Park, IL (1996).

24. J. C. Farmer, G. V. Mack, D. V. Fix, "The Use of Carbon Aerogel Electrodes for Deionizing Water and Treating Aqueous Process Wastes," U. Calif., Lawrence Livermore Natl. Lab. Rept. UCRL-JC-123461 (1996); Intl. J. Environ. Conscious Des. Mfg., Vol. 6, No. 1, in press (1997).

25. A. J. Bard, L. R. Faulkner, "Double-Layer Structure and Adsorbed Intermediates in Electrode Processes," Chapt. 12, Electrochemical Methods, Fundamentals and Applications, John Wiley and Sons, New York, NY, pp. 488-552 (1980).

26. J. S. Newman, "Structure of the Electric Double Layer," Chapt. 7, Electrochemical Systems, 2nd Ed., Prentice Hall, Englewood Cliffs, NJ, pp. 157-185 (1991).

27. J. C. Farmer, S. M. Bahowick, J. E. Harrar, D. V. Fix, R. E. Martinelli, A. K. Vu, K. L. Carroll, "Electrosorption of Chromium Ions on Carbon Aerogel Electrodes as a Means of Remediating Ground Water," U. Calif., Lawrence Livermore Natl. Lab. Rept. UCRL-JC-124565 Rev. 1, August 29 (1996); submitted for publication in special issue of Energy and Fuels (1997).

28. J. A. Trainham, J. Newman, "Flow-Through Porous Electrode Model: Application to Metal-Ion Removal from Dilute Streams," J. Electrochem. Soc., Vol. 124, No. 10, pp. 1528-1540 (1977).

29. Van Zee, J. Newman, "Electrochemical Removal of Silver Ions from Photographic Fixing Solutions Using a Porous Flow-Through Electrode," J. Electrochem. Soc., Vol. 124, No. 5, pp. 706-708 (1977).

30. M. Matlosz, J. Newman, "Experimental Investigation of a Porous Carbon Electrode for the Removal of Mercury from Contaminated Brine," J. Electrochem. Soc., Vol. 133, No. 9, pp. 1850-1859 (1986).

31. D. Pletcher, "Industrial Electrochemistry," Chapter 11, Water Treatment and Environmental Protection, Chapman and Hall, London, UK, p. 291 (1982).

32. Y. Hanzawa, K. Kaneko, R. W. Pekala, M. S. Dresselhaus, "Activated Carbon Aerogels," unpublished manuscript (1996).

33. R. W. Pekala, S. T. Mayer, J. F. Poco, J. L. Kaschmitter, "Structure and Performance of Carbon Aerogel Electrodes," in Novel Forms of Carbon II, C. L. Renschler, D. M. Cox, J. J. Pouch, Y. Achiba, Eds., MRS Symp. Proc., Vol. 349, No. 79 (1994).

34. J. Wang et al., "Carbon Aerogel Composite Electrodes," Anal. Chem., Vol. 65, pp. 2300-2303 (1993).

35. R. W. Pekala, C. T. Alviso, in Novel Forms of Carbon, C. L. Renschler, J. J. Pouch, D. M. Cox, Eds., MRS Symp. Proc., Vol. 270, No. 3 (1992).

36. R. W. Pekala, in Ultrastructure Processing of Advanced Materials, D. R. Uhlmanjn, D. R. Ulrich, Eds., John Wiley and Sons, Inc., New York, NY, pp. 711-717 (1992).

37. S. T. Mayer, R. W. Pekala, J. L. Kaschmitter, "The Aerocapacitor: An Electrochemical Double-layer Energy-Storage Device," J. Electrochemical Society, Vol. 140, No. 2, pp. 446-451 (1993).

38. G. V. Mack, J. C. Farmer, D. V. Fix, G. W. Johnson, D. W. O'Brien, "Design of the Control System for the Continuous-Flow Potential-Swing Capacitive Deionization Process," U. Calif., Lawrence Livermore Natl. Lab. Rept. No. UCRL-ID-117626, September 30 (1994).

39. C. J. King, "Energy Requirements of Separation Processes," Chapt 13, Separation Processes, 2nd Ed., McGraw-Hill Chemical Engineering Series, McGraw-Hill, San Francisco, CA, pp. 660-727 (1980).

40. J. S. Newman, "Activity Coefficients," Chapt. 4, Electrochemical Systems, 2nd Ed., Prentice Hall, Englewood Cliffs, NJ, p. 86-115 (1991).

41. C. O. Bennett, J. E. Myers, "The Overall Energy Balance," Chapt. 4, Momentum, Heat, and Mass Transfer, 2nd Ed., McGraw-Hill Chemical Engineering Series, McGraw-Hill, San Francisco, CA, pp. 40-60 (1974).

42. R. N. Robinson, "Fluid Statics and Dynamics," Chapt. 5. Chemical Engineering Reference Manual, 4th Ed., Professional Publications, Inc., Belmont. CA, pp. 5.1-5.38 (1987).

43. Chemical Engineers' Handbook, 5th Ed., R. H. Perry, C. H. Chilton, Ed., McGraw-Hill, San Francisco, CA (1973).

44. G. Donath, "Aufbereitung von Meerwasser Mit Ionenaustauschern," Vom Wasser, Vol. 61, pp. 237-238 (1983).

45. L. F. Fernandez, J. G. Ibanez, K. Rajeshwar, S. Basak. "The Reduction of Cr(VI) with Polypyrrole on Reticulated Vitreous Carbon: Miscellaneous Effects," 189th Mtg. Electrochem. Soc., Los Angeles, CA, May 5-10, 1996, Abs. 524, Ext. Abs., Vol. 96-1, p. 691.

46. M. Lilga, J. Sukamto, M. Buehler, "Electrically-Controlled Cesium Ion Exchange," Proc. 1996 Annual Technical Exchange Meeting, Efficient Separations and Processing Crosscutting Program, Gathersburg, MD, Jan. 16-19, 1996, pp. 47-52.

47. C. P. Shields, I. Moch, Jr., "Evaluation of Global Seawater Reverse Osmosis Capital and Operating Costs," Technical Paper, 17 pgs., ADA Conference, Monterey, California, August (1996).

48. H. K. Rhee, R. Aris, N. R. Amundson, First-Order Partial Differential Equations: Volume II, Theory and Application of Hyperbolic Systems of Quasilinear Equations, Prentice Hall, Englewood Cliffs, NJ (1986).

49. Zoher Chiba, Lawrence Livermore National Laboratory, 1995, unpublished results.

Table 1. Estimates of Total Energy Requirements for SW Desalination

Process	Heat to Process	Heat to Process	Electrical Power Consumed	Electrical Power Consumed	Total Required Energy
	kJ kg^{-1}	Wh gal^{-1}	kWh m^{-3}	Wh gal^{-1}	Wh gal^{-1}
MSF	290.6	305.6	3.9	14.8	320.3
MED+TVC	290.6	305.6	2.7	10.2	315.8
MED+TVC	193.8	203.8	2.9	11.0	214.8
MVC			11.0	41.6	41.6
MVC			8.0	30.3	30.3
RO+ERT			6.5	24.6	24.6
RO			9.5	36.0	36.0

Note: MSF (multistage flash); MED (multiple effect distillation); TVC (thermo vapor compression); MVC (mechanical vapor compression); RO (reverse osmosis); ERT (energy recovery turbines).

Source: N. M. Wade, "Technical and Economic Evaluation of Distillation and Reverse Osmosis Desalination Processes," Desalination, Vol. 93, pp. 343-363, (1993).

Table 2. Heuristic Estimates of Energy Requirements for Reverse Osmosis

Salt Concentration	Osmotic Pressure	System Category	Pressure (Low)	Pressure (High)	Energy Requirement (Low)	Energy Requirement (High)
ppm	psi		psi	psi	Wh gal^{-1}	Wh gal^{-1}
1000	10	LP	200	300	2.06	3.09
1500	15	LP	200	300	2.06	3.09
2000	20	LP	200	300	2.06	3.09
2500	25	LP	200	300	2.06	3.09
3000	30	LP	200	300	2.06	3.09
3500	35	LP/SP	200	650	2.06	6.69
4000	40	SP	400	650	4.11	6.69
4500	45	SP	400	650	4.11	6.69
5000	50	SP	400	650	4.11	6.69
10000	100	SP	400	650	4.11	6.69
35000	350	SW	800	1500	8.23	15.43

Note: LP (low pressure); SP (standard pressure); SW (sea water). The energy requirement is calculated from the pressure alone and is based on a unit volume of product, with an assumed recovery ratio of 0.70.

Sources: W. J. Conlon, "Membrane Processes," Chapt. 11, Water Quality and Treatment, A Handbook of Community Water Supplies, 4th Ed., R. W. Pontius, Ed., American Water Works Association, McGraw-Hill, San Francisco, CA, pp. 709-746 (1990); R. M. Clark, "Water Supply," Chapt. 5, Standard Handbook of Environmental Engineering, R. A. Corbitt, Ed., McGraw-Hill, San Francisco, CA, pp. 5.146-149 (1989).

Table 3. Estimates of Energy Requirements for Electrodialysis Reversal (EDR)

Salt Concentration	EDR Membrane Stack	EDR Pumping	EDR Total
ppm	Wh gal^{-1}	Wh gal^{-1}	Wh gal^{-1}
1000	2	2.5	4.73
1500	3	2.5	5.78
2000	4	2.5	6.83
2500	5	2.5	7.88
3000	6	2.5	8.93
3500	7	2.5	9.98
4000	8	2.5	11.03
4500	9	2.5	12.08
5000	10	2.5	13.13
10000	20	2.5	23.63
35000	70	2.5	76.13

Source: W. J. Conlon, "Membrane Processes," Chapt. 11, Water Quality and Treatment, A Handbook of Community Water Supplies, 4th Ed., R. W. Pontius, Ed., American Water Works Association, McGraw-Hill, San Francisco, CA, pp. 737 (1990). The total assumes 5% is due to instrumentation.

Table 4. Estimated Energy Requirement for City of Melville Desalting Plant

Plant Feature	RO	EDR
Well Concentration (TDS, ppm)	1600	1600
Feed Concentration (TDS, ppm)	1630	1600
Concentrate Concentration (TDS, ppm)	5300	7500
Product Concentration (TDS, ppm)	60	490
Product-Feed (Recovery) Ratio	0.700	0.842
Feed Capacity (L s^{-1})	23.9	26.5
Product Capacity (L s^{-1})	16.7	22.3
Supply Capacity (L s^{-1})	22.3	22.3
Blending Ratio (Product:Well)	3:1	none
Product Concentration After Blending (TDS, ppm)	445	490
Operating Pressure (kPa/psi)	1,860/270	380/55
Energy Requirement for Pressure Drop Alone (Wh gal^{-1})	2.78	0.47
Capital Cost ($K Canadian)	1,965	1,942
Operating Costs ($ m^3 product)		
Electricity ($0.049 kWh)	0.11	0.10
Chemicals	0.12	0.02
Membrane Replacement	0.08	0.06
Operation & Maintenance	0.04	0.03
Filters, Materials & Spare Parts	0.03	0.03
Total Operating Cost -No Blending ($ m^3 product)	0.38	0.24
Total Operating Cost - With Blending ($ m^3 product)	0.29	0.24
Energy Requirement Based on Electricity (Wh gal^{-1})	8.49	7.71

Source: R. C. Harries, D. Elyanow, D. N. Heshka, K. L. Fischer, "Desalination of Brackish Groundwater for a Prarie Community Using Electrodialysis Reversal," Desalination, Vol. 84, pp. 109-121, (1991). The value of 7.71 Wh gal^{-1} for EDR is higher than that estimated with the heuristic rule, which is 5.99 Wh gal^{-1}.

Table 6a. Conditions for Six Different Cases with Feed Concentration of 2000 ppm (Fixed C_p & R; Variable h).

Parameter Description	Case 1: 1.2 V & 100 ml min^{-1} $stack^{-1}$	Case 2: 1.2 V & 25 ml min^{-1} $stack^{-1}$	Case 3: 1.2 V & 10 ml min^{-1} $stack^{-1}$	Case 4: 0.6 V & 10 ml min^{-1} $stack^{-1}$	Case 5: 1.3 V & 10 ml min^{-1} $stack^{-1}$	Case 6: increased CAC density
Voltage	1.20	1.20	1.20	0.60	1.30	1.30
Channel Flow (ml min^{-1})	100.00	25.00	10.00	10.00	10.00	10.00
Channel Flow (gal min^{-1})	2.65	0.66	0.26	0.26	0.26	0.26
Breakthrough Time (min)	120.00	120.00	120.00	120.00	120.00	60.00
CAC per Channel (ft^2) @ 2000 ppm	459.914	78.192	24.240	157.776	19.525	1.009
CAC Thickness (in)	$1.00x10^{-02}$	$1.00x10^{-02}$	$1.00x10^{-02}$	$1.00x10^{-02}$	$1.00x10^{-02}$	$5.00x10^{-02}$
CAC Sp. Gr.	0.413	0.413	0.413	0.413	0.413	0.800
Channel Length (ft)	689.87	117.29	36.36	236.66	29.29	1.51
Channel Height (in)	$5.27x10^{-03}$	$1.57x10^{-02}$	$2.51x10^{-02}$		$3.52x10^{-02}$	$1.95x10^{-02}$
Channel Width (in)	4.00	4.00	4.00	4.00	4.00	4.00
Reynolds Number	33.37	8.32	3.32	3.35	3.31	3.32
Moody Friction Factor	1.11	3.07	5.99	5.95	6.00	5.99
Pressure Drop (psi)	$9.50x10^{+02}$	1.06	$2.50x10^{-02}$		$7.32x10^{-03}$	$2.23x10^{-03}$
Energy Recovery (%)	50	50	50	50	50	70
Energy (Wh gal^{-1}) - No Depletion	4.218	3.054	2.592		2.474	0.770
Energy (Wh gal^{-1}) - With Depletion	1.343	1.613	2.510		2.567	1.011
Product-Feed Ratio	0.500	0.500	0.500	0.500	0.500	0.850
Product Concentration (ppm)	100	100	100	100	100	100
Production (GPD per Channel)	19.021	4.755	1.902		1.902	3.234
Production (GPD per 4000 ft^2)	165	243	314		390	12817
CAC Required for 5 MGPD (ft^2)	120,897,704	82,216,898	63,720,335		51,325,943	1,560,401

Note: This series of calculations assumes a fixed minimum product concentration of 100 ppm and a fixed recovery (product/feed) ratio. The recovery ratio in Cases 1 through 5 was assumed to be 0.5, whereas a value of 0.85 was assumed in Case 6. The electrode gap was calculated based upon these fixed values, as well as the feed concentration, the density and thickness of the CAC sheets, and the electrosorption capacity. Cases with recovery ratios less than 0.5 are not listed (shaded areas). The "Energy (Requirement) - No Depletion" assumes that the electroactive species responsible for the parasitic current is generated in situ and not depleted, whereas the "Energy (Requirement) - With Depletion" assumes that the electroactive species is introduced in the feed (dissolved oxygen, etc.) and is depleted by the parasitic electrode reaction. The channel is treated like a tubular reactor. Note that some reasonably attractive cases for brackish water were found, but that no good combination of parameters for sea water was found. Computational results for other feed concentrations are summarized in Tables 6b through 6f, as well as in Figures 6a through 6f.

Table 6b. Electrode Gap (in) vs. Feed Concentration for Conditions in Table 6a.

Feed Conc. (ppm)	Case 1: 1.2 V & 100 ml min^{-1} $stack^{-1}$	Case 2: 1.2 V & 25 ml min^{-1} $stack^{-1}$	Case 3: 1.2 V & 10 ml min^{-1} $stack^{-1}$	Case 4: 0.6 V & 10 ml min^{-1} $stack^{-1}$	Case 5: 1.3 V & 10 ml min^{-1} $stack^{-1}$	Case 6: increased CAC density
1000	$2.174x10^{-02}$	$3.990x10^{-02}$	$5.637x10^{-02}$		$7.405x10^{-02}$	$8.571x10^{-02}$
1500	$1.089x10^{-02}$	$2.393x10^{-02}$	$3.577x10^{-02}$		$4.848x10^{-02}$	$4.205x10^{-02}$
2000	$5.270x10^{-03}$	$1.567x10^{-02}$	$2.511x10^{-02}$		$3.525x10^{-02}$	$1.946x10^{-02}$
2500	$1.771x10^{-03}$	$1.053x10^{-02}$	$1.847x10^{-02}$		$2.700x10^{-02}$	$5.390x10^{-03}$
3000		$6.973x10^{-03}$	$1.389x10^{-02}$		$2.131x10^{-02}$	
3500		$4.350x10^{-03}$	$1.050x10^{-02}$		$1.710x10^{-02}$	
4000		$2.323x10^{-03}$	$7.887x10^{-03}$		$1.386x10^{-02}$	
4500		$7.040x10^{-04}$	$5.798x10^{-03}$		$1.127x10^{-02}$	
5000			$4.085x10^{-03}$		$9.139x10^{-03}$	
10000						
35000						

Table 6c. Channel Length (ft) vs. Feed Concentration for Conditions in Table 6a.

Feed Conc. (ppm)	Case 1: 1.2 V & 100 ml min^{-1} $stack^{-1}$	Case 2: 1.2 V & 25 ml min^{-1} $stack^{-1}$	Case 3: 1.2 V & 10 ml min^{-1} $stack^{-1}$	Case 4: 0.6 V & 10 ml min^{-1} $stack^{-1}$	Case 5: 1.3 V & 10 ml min^{-1} $stack^{-1}$	Case 6: increased CAC density
1000	395.359	67.216	20.838		16.785	0.867
1500	550.149	93.533	28.996		23.356	1.207
2000	689.871	117.287	36.360		29.288	1.514
2500	819.579	139.339	43.197		34.794	1.798
3000		160.140	49.645		39.988	
3500		179.962	55.790		44.938	
4000		198.988	61.688		49.689	
4500		217.348	67.380		54.274	
5000			72.895		58.716	
10000						
35000						

Table 6d. Pressure Drop (psi) vs. Feed Concentration for Conditions in Table 6a.

Feed Conc. (ppm)	Case 1: 1.2 V & 100 ml min^{-1} $stack^{-1}$	Case 2: 1.2 V & 25 ml min^{-1} $stack^{-1}$	Case 3: 1.2 V & 10 ml min^{-1} $stack^{-1}$	Case 4: 0.6 V & 10 ml min^{-1} $stack^{-1}$	Case 5: 1.3 V & 10 ml min^{-1} $stack^{-1}$	Case 6: increased CAC density
1000	7.81	$3.72x10^{-02}$	$1.28x10^{-03}$		$4.60x10^{-04}$	$1.54x10^{-05}$
1500	$8.61x10^{+01}$	$2.38x10^{-01}$	$6.93x10^{-03}$		$2.26x10^{-03}$	$1.78x10^{-04}$
2000	$9.50x10^{+02}$	1.06	$2.50x10^{-02}$		$7.32x10^{-03}$	$2.23x10^{-03}$
2500	$2.97x10^{+04}$	4.14	$7.44x10^{-02}$		$1.93x10^{-02}$	$1.24x10^{-01}$
3000		$1.64x10^{+01}$	$2.01x10^{-01}$		$4.50x10^{-02}$	
3500		$7.57x10^{+01}$	$5.22x10^{-01}$		$9.75x10^{-02}$	
4000		$5.49x10^{+02}$	1.36		$2.02x10^{-01}$	
4500		$2.15x10^{+04}$	3.74		$4.11x10^{-01}$	
5000			$1.15x10^{+01}$		$8.33x10^{-01}$	
10000						
35000						

Table 6e. Energy Required (Wh gal^{-1}) vs. Feed Concentration - Table 6a - No Depletion.

Feed Conc. (ppm)	Case 1: 1.2 V & 100 ml min^{-1} stack^{-1}	Case 2: 1.2 V & 25 ml min^{-1} stack^{-1}	Case 3: 1.2 V & 10 ml min^{-1} stack^{-1}	Case 6: increased CAC density	Stored Energy ~1/2 QV @ 1.2 V	Minimum Theoretical @ R=0.5
1000	2.211	1.657	1.395	0.538	0.937	0.0412
1500	3.165	2.377	2.010	0.640	1.458	0.0677
2000	4.218	3.054	2.592	0.770	1.979	0.0946
2500	11.022	3.701	3.152	0.914	2.500	0.1217
3000		4.329	3.694		3.021	0.1488
3500		4.949	4.224		3.541	0.1760
4000		5.642	4.743		4.062	0.2032
4500		10.580	5.253		4.583	0.2305
5000			5.757		5.104	0.2579
10000					10.311	0.5338
35000					36.350	1.9895

Table 6f. Energy Required (Wh gal^{-1}) vs. Feed Concentration - Table 6a - With Depletion.

Feed Conc. (ppm)	Case 1: 1.2 V & 100 ml min^{-1} stack^{-1}	Case 2: 1.2 V & 25 ml min^{-1} stack^{-1}	Case 3: 1.2 V & 10 ml min^{-1} stack^{-1}	Case 6: increased CAC density	Stored Energy ~1/2 QV @ 1.2 V	Minimum Theoretical @ R=0.5
1000	0.693	1.027	1.445	0.543	0.937	0.0412
1500	0.919	1.350	2.099	0.707	1.458	0.0677
2000	1.343	1.613	2.510	1.011	1.979	0.0946
2500	7.577	1.873	2.802	1.806	2.500	0.1217
3000		2.135	3.065		3.021	0.1488
3500		2.408	3.325		3.541	0.1760
4000		2.766	3.585		4.062	0.2032
4500		7.382	3.845		4.583	0.2305
5000			4.107		5.104	0.2579
10000					10.311	0.5338
35000					36.350	1.9895

Table 7a. Conditions for Six Different Cases with Feed Concentration of 2000 ppm (Fixed h; Variable C_p & R).

Parameter Description	Case 1: 1.2 V & 100 ml min^{-1} $stack^{-1}$	Case 2: 1.2 V & 25 ml min^{-1} $stack^{-1}$	Case 3: 1.2 V & 10 ml min^{-1} $stack^{-1}$	Case 4: 0.6 V & 10 ml min^{-1} $stack^{-1}$	Case 5: Case 3 with smaller gap	Case 6: increased CAC density
Voltage	1.20	1.20	1.20	0.60	1.20	1.30
Channel Flow (ml min^{-1})	100.00	25.00	10.00	10.00	10.00	10.00
Channel Flow (gal min^{-1})	2.65	0.66	0.26	0.26	0.26	0.26
Breakthrough Time (min)	120.00	120.00	120.00	120.00	120.00	60.00
CAC per Channel (ft^2) @ 2000 ppm	231.103	57.776	23.110	23.110	23.222	0.970
CAC Thickness (in)	$1.00x10^{-02}$	$1.00x10^{-02}$	$1.00x10^{-02}$	$1.00x10^{-02}$	$1.00x10^{-02}$	$5.00x10^{-02}$
CAC Sp. Gr.	0.413	0.413	0.413	0.413	0.413	0.800
Channel Length (ft)	346.65	86.66	34.67	34.67	34.83	1.45
Channel Height - Electrode Gap (in)	$2.72x10^{-02}$	$2.72x10^{-02}$	$2.72x10^{-02}$	$2.72x10^{-02}$	$1.00x10^{-02}$	$1.38x10^{-02}$
Channel Width (in)	4.00	4.00	4.00	4.00	4.00	4.00
Reynolds Number	33.18	8.30	3.32	3.32	3.33	3.33
Moody Friction Factor	1.12	3.07	6.00	6.00	5.98	5.98
Pressure Drop (psi)	3.52	$1.51x10^{-01}$	$1.89x10^{-02}$	$1.89x10^{-02}$	$3.77x10^{-01}$	$6.03x10^{-03}$
Energy Recovery (%)	50	50	50	50	50	70
Energy (Wh gal^{-1}) - No Depletion	2.023	2.258	2.472	0.381	2.480	0.725
Energy (Wh gal^{-1}) - With Depletion	0.742	1.345	2.444	0.821	2.502	1.063
Product-Feed Ratio	0.500	0.500	0.500	0.500	0.620	0.863
Product Concentration (ppm)	1045	596	189	1722	180	174
Production (GPD per Channel)	19.021	4.755	1.902	1.902	2.359	3.283
Production (GPD per 4000 ft^2)	329	329	329	329	406	13541
CAC Required for 5 MGPD (ft^2)	60,749,960	60,749,960	60,749,960	60,749,960	49,228,358	1,476,960

Note: A fixed electrode gap of 0.027 inches was assumed in Cases 1 through 4, whereas gaps of 0.010 and 0.014 inches were assumed in Cases 5 and 6, respectively. The *maximum possible recovery ratio and the minimum possible product concentration were estimated based upon the fixed electrode gap, as well as the feed concentration, the density and thickness of the CAC sheets, and the electrosorption capacity. The "Energy (Requirement) - No Depletion" assumes that the electroactive species responsible for the parasitic current is generated in situ and not depleted, whereas the "Energy (Requirement) - With Depletion" assumes that the electroactive species is introduced in the feed (dissolved oxygen, etc.) and is depleted by the parasitic electrode reaction. The channel is treated like a tubular reactor. Note that some reasonably attractive cases for brackish water were found, but that no good combination of parameters for sea water was found. Computational results for other feed concentrations are summarized in Tables 7b through 7i, as well as in Figures 7a through 7f.*

Table 7b. Minimum Product Concentration (ppm) vs. Feed Concentration - Table 7a.

Feed Conc. (ppm)	Case 1: 1.2 V & 100 ml min^{-1} $stack^{-1}$	Case 2: 1.2 V & 25 ml min^{-1} $stack^{-1}$	Case 3: 1.2 V & 10 ml min^{-1} $stack^{-1}$	Case 4: 0.6 V & 10 ml min^{-1} $stack^{-1}$	Case 5: Case 3 with smaller gap	Case 6: increased CAC density
1000	211	226	194	770	182	173
1500	618	203	211	1243	179	186
2000	1045	596	189	1722	180	174
2500	1485	1007	574	2204	185	171
3000	1933	1431	975	2689	172	178
3500	2387	1863	1387	3175	199	167
4000	2845	2301	1808	3663	407	189
4500	3307	2746	2236	4152	789	182
5000	3772	3194	2670	4642	1180	199
10000	8514	7815	7181	9567	5378	191
35000	32903	31917	31022	34389	28478	9742

Table 7c. Maximum Recovery (Product/Feed) Ratio vs. Feed Concentration - Table 7a.

Feed Conc. (ppm)	Case 1: 1.2 V & 100 ml min^{-1} $stack^{-1}$	Case 2: 1.2 V & 25 ml min^{-1} $stack^{-1}$	Case 3: 1.2 V & 10 ml min^{-1} $stack^{-1}$	Case 4: 0.6 V & 10 ml min^{-1} $stack^{-1}$	Case 5: Case 3 with smaller gap	Case 6: increased CAC density
1000	0.500	0.600	0.650	0.500	0.750	0.920
1500	0.500	0.500	0.565	0.500	0.675	0.890
2000	0.500	0.500	0.500	0.500	0.620	0.863
2500	0.500	0.500	0.500	0.500	0.577	0.840
3000	0.500	0.500	0.500	0.500	0.540	0.820
3500	0.500	0.500	0.500	0.500	0.512	0.801
4000	0.500	0.500	0.500	0.500	0.500	0.785
4500	0.500	0.500	0.500	0.500	0.500	0.769
5000	0.500	0.500	0.500	0.500	0.500	0.755
10000	0.500	0.500	0.500	0.500	0.500	0.646
35000	0.500	0.500	0.500	0.500	0.500	0.500

Table 7d. Channel Length (ft) vs. Feed Concentration for Conditions in Table 7a.

Feed Conc. (ppm)	Case 1: 1.2 V & 100 ml min^{-1} $stack^{-1}$	Case 2: 1.2 V & 25 ml min^{-1} $stack^{-1}$	Case 3: 1.2 V & 10 ml min^{-1} $stack^{-1}$	Case 4: 0.6 V & 10 ml min^{-1} $stack^{-1}$	Case 5: Case 3 with smaller gap	Case 6: increased CAC density
1000	346.654	57.776	18.666	34.665	18.944	0.797
1500	346.654	86.663	26.689	34.665	27.364	1.133
2000	346.654	86.663	34.665	34.665	34.833	1.455
2500	346.654	86.663	34.665	34.665	41.664	1.745
3000	346.654	86.663	34.665	34.665	48.413	2.011
3500	346.654	86.663	34.665	34.665	54.168	2.277
4000	346.654	86.663	34.665	34.665	56.832	2.510
4500	346.654	86.663	34.665	34.665	56.832	2.753
5000	346.654	86.663	34.665	34.665	56.832	2.974
10000	346.654	86.663	34.665	34.665	56.832	5.021
35000	346.654	86.663	34.665	34.665	56.832	9.163

Table 7e. Pressure Drop (psi) vs. Feed Concentration for Conditions in Table 7a.

Feed Conc. (ppm)	Case 1: 1.2 V & 100 ml min^{-1} $stack^{-1}$	Case 2: 1.2 V & 25 ml min^{-1} $stack^{-1}$	Case 3: 1.2 V & 10 ml min^{-1} $stack^{-1}$	Case 4: 0.6 V & 10 ml min^{-1} $stack^{-1}$	Case 5: Case 3 with smaller gap	Case 6: increased CAC density
1000	3.52	$1.01x10^{-01}$	$1.02x10^{-02}$	$1.89x10^{-02}$	$2.05x10^{-01}$	$3.30x10^{-03}$
1500	3.52	$1.51x10^{-01}$	$1.45x10^{-02}$	$1.89x10^{-02}$	$2.96x10^{-01}$	$4.69x10^{-03}$
2000	3.52	$1.51x10^{-01}$	$1.89x10^{-02}$	$1.89x10^{-02}$	$3.77x10^{-01}$	$6.03x10^{-03}$
2500	3.52	$1.51x10^{-01}$	$1.89x10^{-02}$	$1.89x10^{-02}$	$4.51x10^{-01}$	$7.23x10^{-03}$
3000	3.52	$1.51x10^{-01}$	$1.89x10^{-02}$	$1.89x10^{-02}$	$5.24x10^{-01}$	$8.34x10^{-03}$
3500	3.52	$1.51x10^{-01}$	$1.89x10^{-02}$	$1.89x10^{-02}$	$5.86x10^{-01}$	$9.43x10^{-03}$
4000	3.52	$1.51x10^{-01}$	$1.89x10^{-02}$	$1.89x10^{-02}$	$6.15x10^{-01}$	$1.04x10^{-02}$
4500	3.52	$1.51x10^{-01}$	$1.89x10^{-02}$	$1.89x10^{-02}$	$6.15x10^{-01}$	$1.14x10^{-02}$
5000	3.52	$1.51x10^{-01}$	$1.89x10^{-02}$	$1.89x10^{-02}$	$6.15x10^{-01}$	$1.23x10^{-02}$
10000	3.52	$1.51x10^{-01}$	$1.89x10^{-02}$	$1.89x10^{-02}$	$6.15x10^{-01}$	$2.08x10^{-02}$
35000	3.52	$1.51x10^{-01}$	$1.89x10^{-02}$	$1.89x10^{-02}$	$6.15x10^{-01}$	$3.80x10^{-02}$

Table 7f. Minimum Energy Requirement (Wh gal^{-1}) vs. Feed Concentration - Table 7a.

Feed Conc. (ppm)	Case 1: 1.2 V & 100 ml min^{-1} stack^{-1}	Case 2: 1.2 V & 25 ml min^{-1} stack^{-1}	Case 3: 1.2 V & 10 ml min^{-1} stack^{-1}	Case 4: 0.6 V & 10 ml min^{-1} stack^{-1}	Case 5: Case 3 with smaller gap	Case 6: increased CAC density
1000	0.030	0.032	0.038	0.002	0.046	0.076
1500	0.023	0.055	0.058	0.002	0.072	0.112
2000	0.019	0.044	0.082	0.002	0.096	0.149
2500	0.017	0.039	0.068	0.001	0.118	0.183
3000	0.016	0.035	0.061	0.001	0.143	0.214
3500	0.015	0.032	0.055	0.001	0.162	0.247
4000	0.014	0.030	0.051	0.001	0.159	0.274
4500	0.013	0.028	0.048	0.001	0.144	0.305
5000	0.012	0.027	0.045	0.001	0.133	0.331
10000	0.009	0.019	0.032	0.001	0.089	0.603
35000	0.055	0.012	0.020	0.000	0.053	0.859

Table 7g. Stored Electrical Energy ~ 1/2 QV (Wh gal^{-1}) vs. Feed Concentration - Table 7a.

Feed Conc. (ppm)	Case 1: 1.2 V & 100 ml min^{-1} stack^{-1}	Case 2: 1.2 V & 25 ml min^{-1} stack^{-1}	Case 3: 1.2 V & 10 ml min^{-1} stack^{-1}	Case 4: 0.6 V & 10 ml min^{-1} stack^{-1}	Case 5: Case 3 with smaller gap	Case 6: increased CAC density
1000	0.822	0.806	0.840	0.120	0.852	0.9328
1500	0.919	1.351	1.342	0.134	1.376	1.4821
2000	0.994	1.462	1.887	0.145	1.896	2.0603
2500	1.057	1.555	2.006	0.154	2.411	2.6284
3000	1.112	1.635	2.109	0.162	2.946	3.1847
3500	1.160	1.705	2.200	0.169	3.438	3.7604
4000	1.203	1.769	2.283	0.175	3.742	4.3005
4500	1.243	1.827	2.358	0.181	3.865	4.8718
5000	1.279	1.881	2.427	0.186	3.979	5.4175
10000	1.548	2.276	2.936	0.226	4.814	11.0685
35000	2.184	3.211	4.143	0.318	6.793	28.5003

Table 7h. Energy Required (Wh gal^{-1}) vs. Feed Concentration - Table 7a - No Depletion.

Feed Conc. (ppm)	Case 1: 1.2 V & 100 ml min^{-1} stack^{-1}	Case 2: 1.2 V & 25 ml min^{-1} stack^{-1}	Case 3: 1.2 V & 10 ml min^{-1} stack^{-1}	Case 4: 0.6 V & 10 ml min^{-1} stack^{-1}	Case 5: Case 3 with smaller gap	Case 6: increased CAC density
1000	1.939	1.422	1.245	0.369	1.260	0.3461
1500	1.986	2.203	1.849	0.376	1.892	0.5320
2000	2.023	2.258	2.472	0.381	2.480	0.7249
2500	2.054	2.304	2.531	0.386	3.038	0.9123
3000	2.081	2.343	2.582	0.389	3.602	1.0943
3500	2.105	2.378	2.627	0.393	4.101	1.2820
4000	2.127	2.410	2.668	0.396	4.370	1.4568
4500	2.146	2.439	2.705	0.399	4.431	1.6416
5000	2.164	2.466	2.740	0.402	4.488	1.8173
10000	2.298	2.662	2.993	0.421	4.905	3.6217
35000	2.616	3.129	3.595	0.467	5.893	9.0503

Table 7i. Energy Required (Wh gal^{-1}) vs. Feed Concentration - Table 7a - With Depletion.

Feed Conc. (ppm)	Case 1: 1.2 V & 100 ml min^{-1} stack^{-1}	Case 2: 1.2 V & 25 ml min^{-1} stack^{-1}	Case 3: 1.2 V & 10 ml min^{-1} stack^{-1}	Case 4: 0.6 V & 10 ml min^{-1} stack^{-1}	Case 5: Case 3 with smaller gap	Case 6: increased CAC density
1000	0.657	0.970	1.716	0.809	1.969	0.5477
1500	0.705	1.290	2.107	0.815	2.241	0.8060
2000	0.742	1.345	2.444	0.821	2.502	1.0634
2500	0.774	1.391	2.503	0.825	2.760	1.3048
3000	0.801	1.431	2.554	0.829	3.027	1.5330
3500	0.825	1.466	2.599	0.832	3.273	1.7639
4000	0.847	1.498	2.640	0.836	3.425	1.9744
4500	0.866	1.527	2.677	0.838	3.487	2.1943
5000	0.884	1.554	2.712	0.841	3.543	2.4000
10000	1.019	1.750	2.965	0.860	3.960	4.4130
35000	1.336	2.218	3.568	0.907	4.949	9.9963

Table 8. A Comparison of Desalination Processes for Brackish Water

	EDR	RO	CAC CDI	CAC CDI
Source	Tables 3 & 4	Tables 2 & 4	Table 7 - Case 3	Table 7 - Case 6
Feed Concentration (ppm)	1600	1630	1500/2000	1500/2000
Product Concentration (ppm)	490	60	211/189	186/174
Recovery (Product/Feed) Ratio	0.842	0.700	0.565/0.500	0.890/0.863
Pressure Differential (psi)	55	270	1.89/1.89x10^{-3}	4.69/6.03x10^{-3}
Energy Requirement (Wh gal^{-1}) - Lowest	5.78-6.83	2.06-3.09	1.85/2.47	0.53/0.73
Energy Requirement (Wh gal^{-1}) - Highest	7.71	8.49	2.11/2.44	0.81/1.06

Figure Captions

Figure 1. Electrosorption of Na^+ and Cl^- ions on 54 double-sided CAC electrodes. Results for 100, 500 and 1000 mS cm^{-1}.

Figure 2. Electrosorption of Na+ and Cl- on 100 double-sided electrodes. Results for 0.6 and 1.2 V compared.

Figure 3. Electrosorption capacity for NaCl on carbon aerogel composite (CAC) electrodes. Comparison of first regression analysis (Equation 5) to experimental data.

Figure 4. Electrosorption capacity for NaCl on carbon aerogel composite (CAC) electrodes. Comparison of second regression analysis (Equation 6) to experimental data.

Figure 5. Moody friction factor, based upon measured pressure drop, correlated with Reynolds number.

Figure6a. Assumed recovery ratios (0.50 or 0.85) at various feed concentrations, for Cases 1 through 6 given in Table 6a.

Figure 6b. Calculated electrode gap (channel height) at various feed concentrations, for Cases 1 through 6 given in Table 6a. Note that Table 6a only provides the value at 2000 ppm.

Figure 6c. Calculated energy requirements at various feed concentrations, for Cases 1 through 6 given in Table 6a. These estimates assume no depletion of electroactive species responsible for parasitic current and are therefore considered a "worst case" scenario.

Figure 6d. Calculated energy requirements shown in Figure 6c with magnified scale.

Figure 6e. Calculated energy reuirements at various feed concentrations, for Cases 1 through 6 given in Table 6a. These estimates assume that electroactive species responsible for parasitic current are introduced in the feed and are therefore depleted, a "best case" scenario.

Figure 6f. Calculated energy requirements shown in Figure 6e with magnified scale.

Figure 7a. Estimates of the maximum possible recovery (product/feed) ratios at various feed concentrations, for cases 1 through 6 given in Table 7a.

Figure 7b. Estimates of the minimum possible salt concentration in the product at various feed concentrations, for Cases 1 through 6 given in Table 7a.

Figure 7c. Calculated theoretical minimum energy requirement for separation of feed into product and concentrate. Values at various feed concentrations, for Cases 1 through 6 given in Table 7a.

Figure 7d. Calculated energy storage during separation of feed into product and concentrate. Values at various feed concentrations, for Cases 1 through 6 given in Table 7a.

Figure 7e. Calculated energy requirements at various feed concentrations, for cases 1 through 6 given in Table 7a. These estimates assume that electroactive species responsible for parasitic current are introduced in the feed and are therefore depleted, a "best case" scenario.

Figure 7f. Calculated energy requirement at various feed concentrations, for Cases 1 through 6 given in Table 6a. These estimates assume no depletion of electroactive species responsible for parasitic current and are therefore considered a "worst case" scenario.

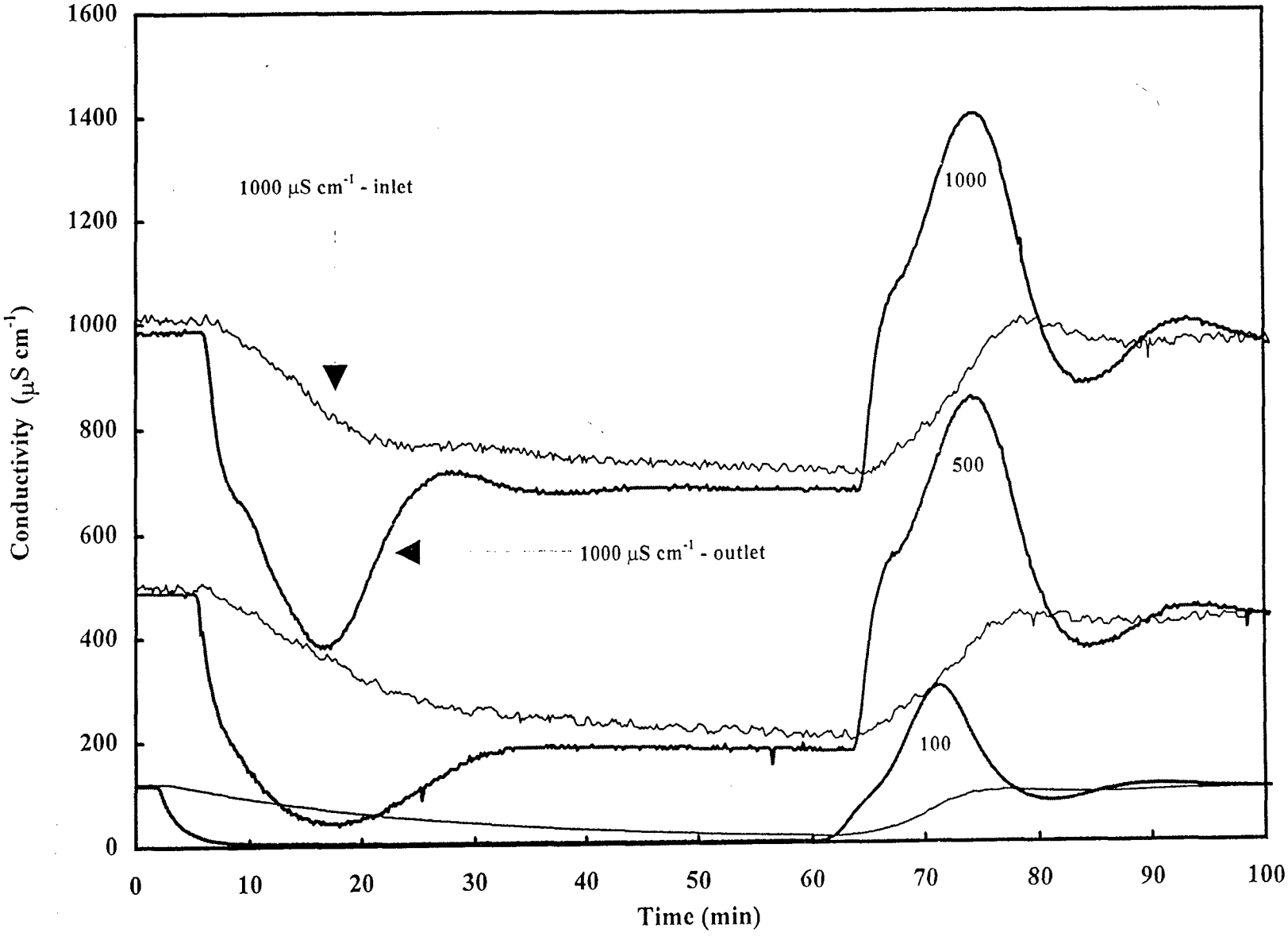
1600
1400
1200
1000
800
600
400
200
0
Conductivity (μS cm-1)
0
10
20
30
40
50
60
70
80
90
100
Time (min)
1000 μS cm-1 - inlet
1000 μS cm-1 - outlet
1000
500
100

Figure 1

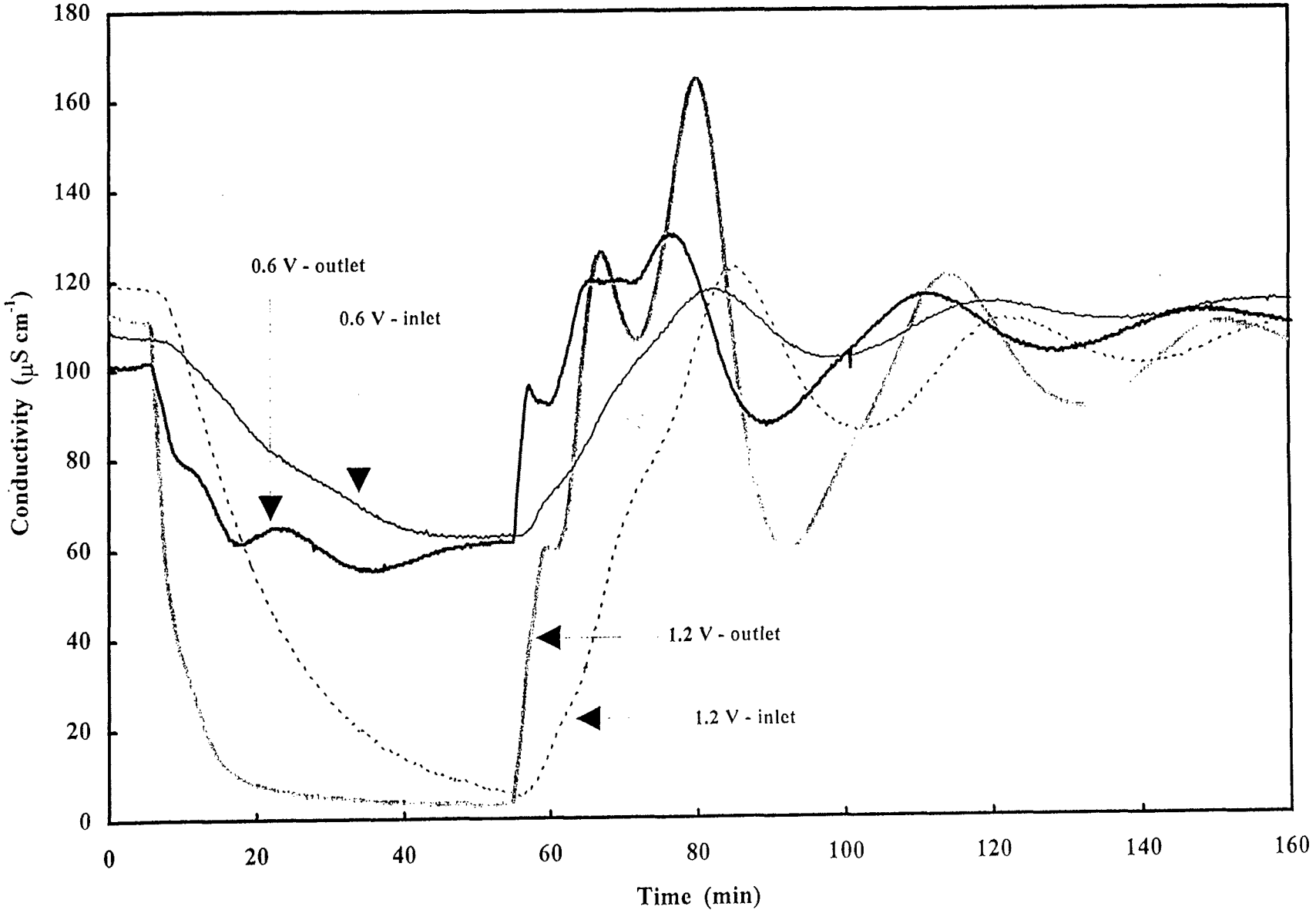
180
160
140
120
100
80
60
40
20
0
Conductivity (μS cm-1)
0.6 V - outlet
0.6 V - inlet
1.2 V - outlet
1.2 V - inlet
0
20
40
60
80
100
120
140
160
Time (min)

Figure 2

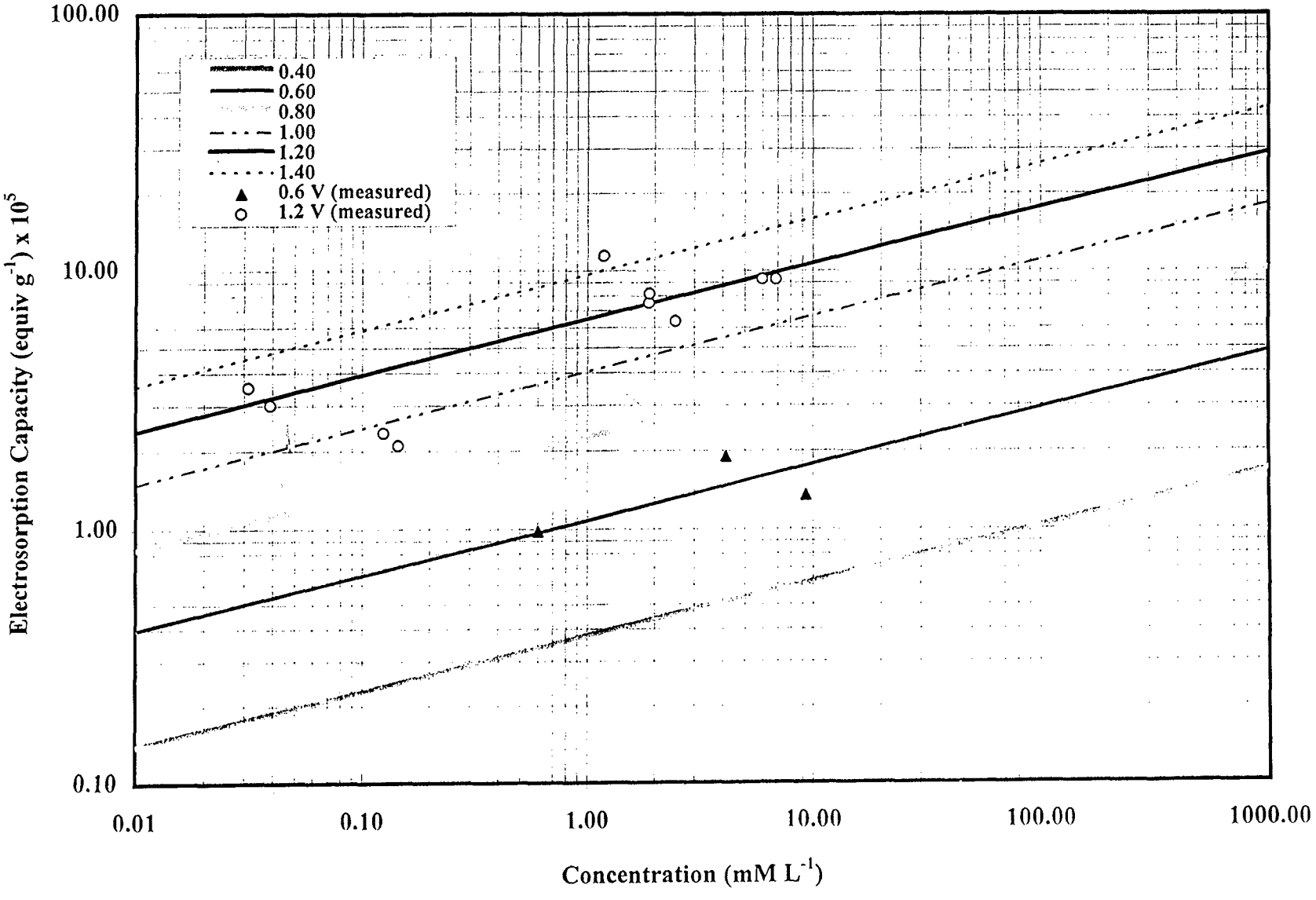
100.00
10.00
1.00
0.10
0.01
0.10
1.00
10.00
100.00
1000.00
Electrosorption Capacity (equiv g^{-1}) x 10^{5}
Concentration (mM L^{-1})
0.40
0.60
0.80
1.00
1.20
1.40
0.6 V (measured)
1.2 V (measured)

Figure 3

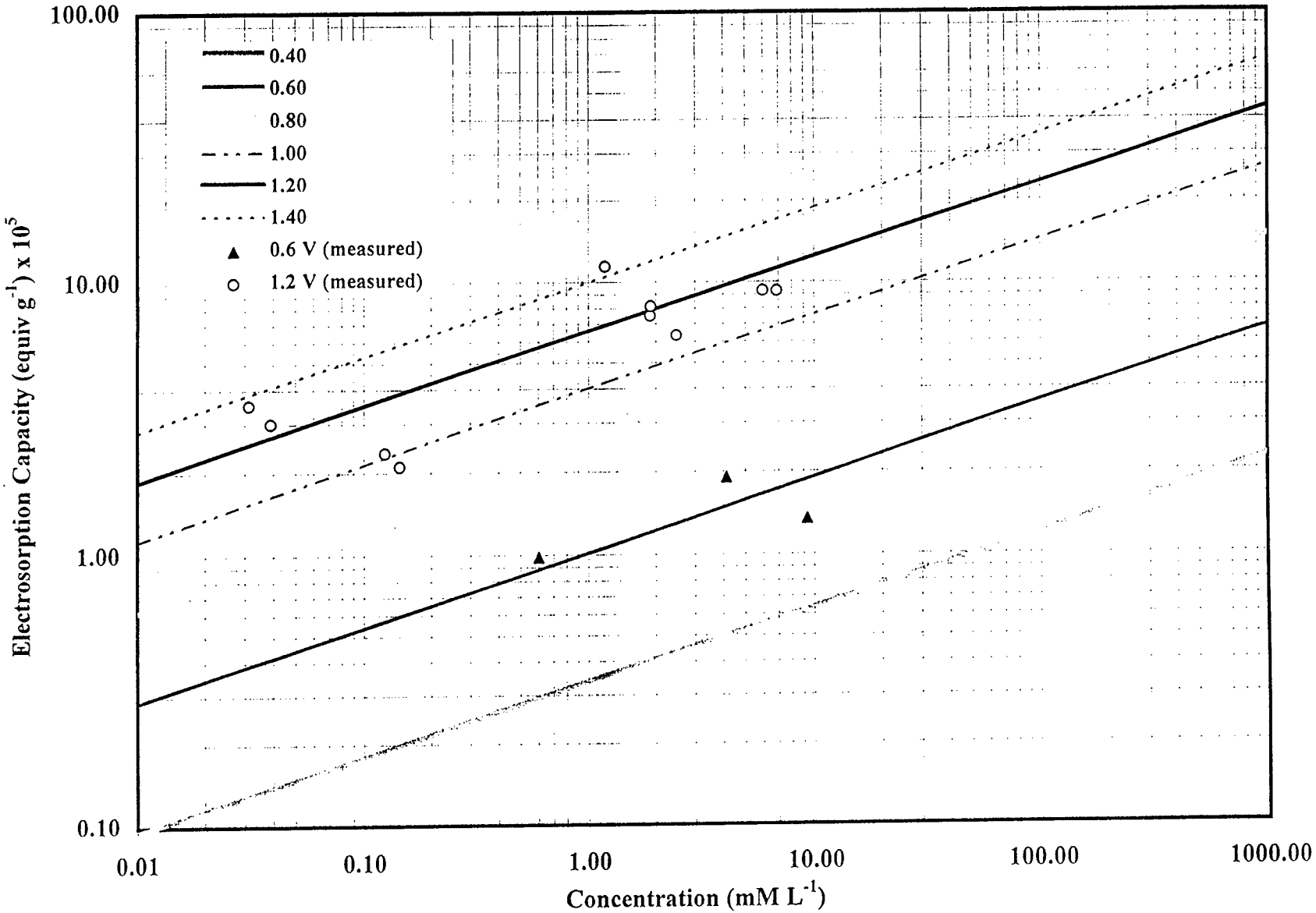
100.00
10.00
1.00
0.10
0.01
0.10
1.00
10.00
100.00
1000.00
Electrosorption Capacity (equiv g^{-1}) x 10^{5}
Concentration (mM L^{-1})
0.40
0.60
0.80
1.00
1.20
1.40
0.6 V (measured)
1.2 V (measured)

Figure 4

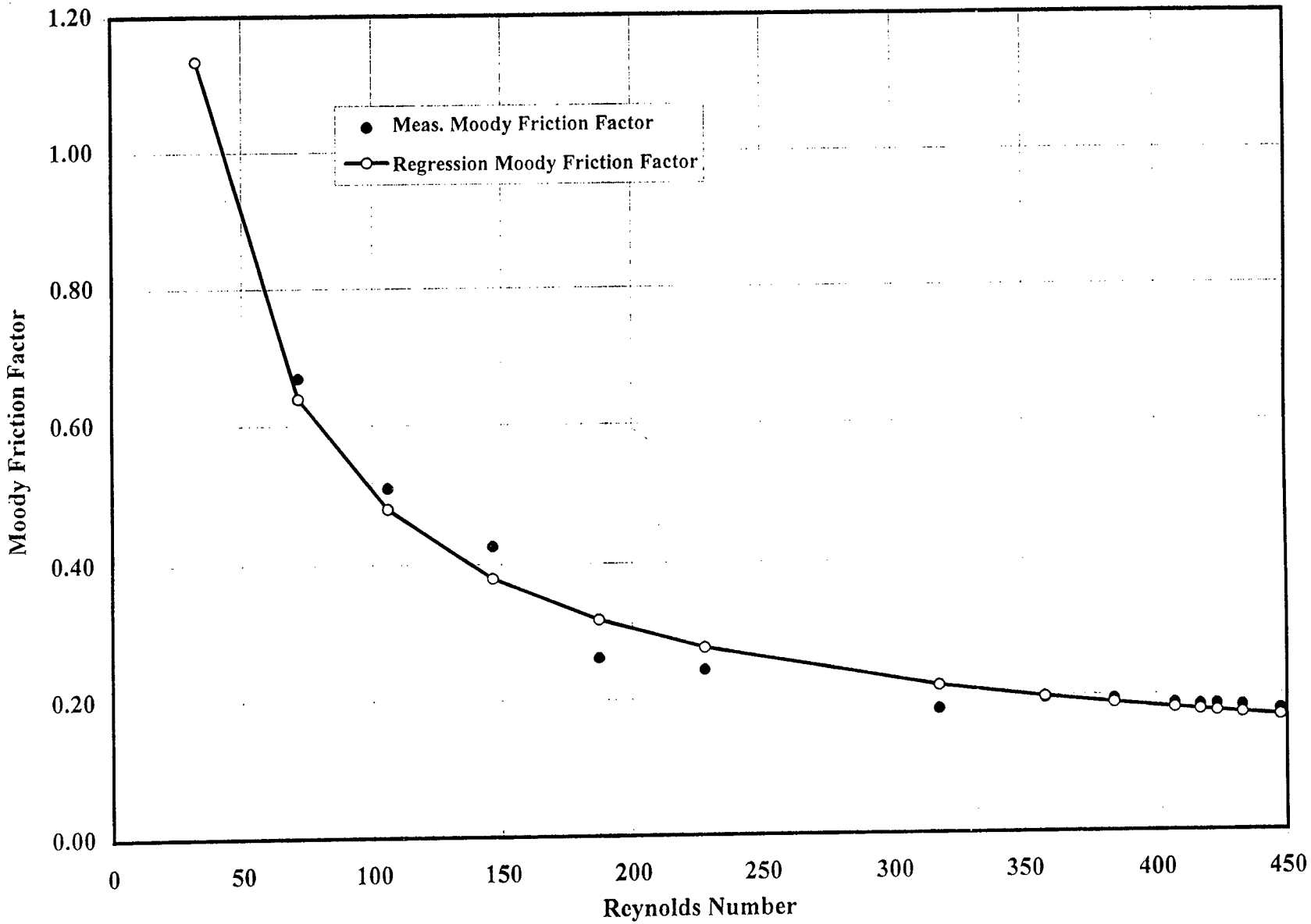
Meas. Moody Friction Factor
Regression Moody Friction Factor
Moody Friction Factor
1.20
1.00
0.80
0.60
0.40
0.20
0.00
0
50
100
150
200
250
300
350
400
450
Reynolds Number

Figure 5

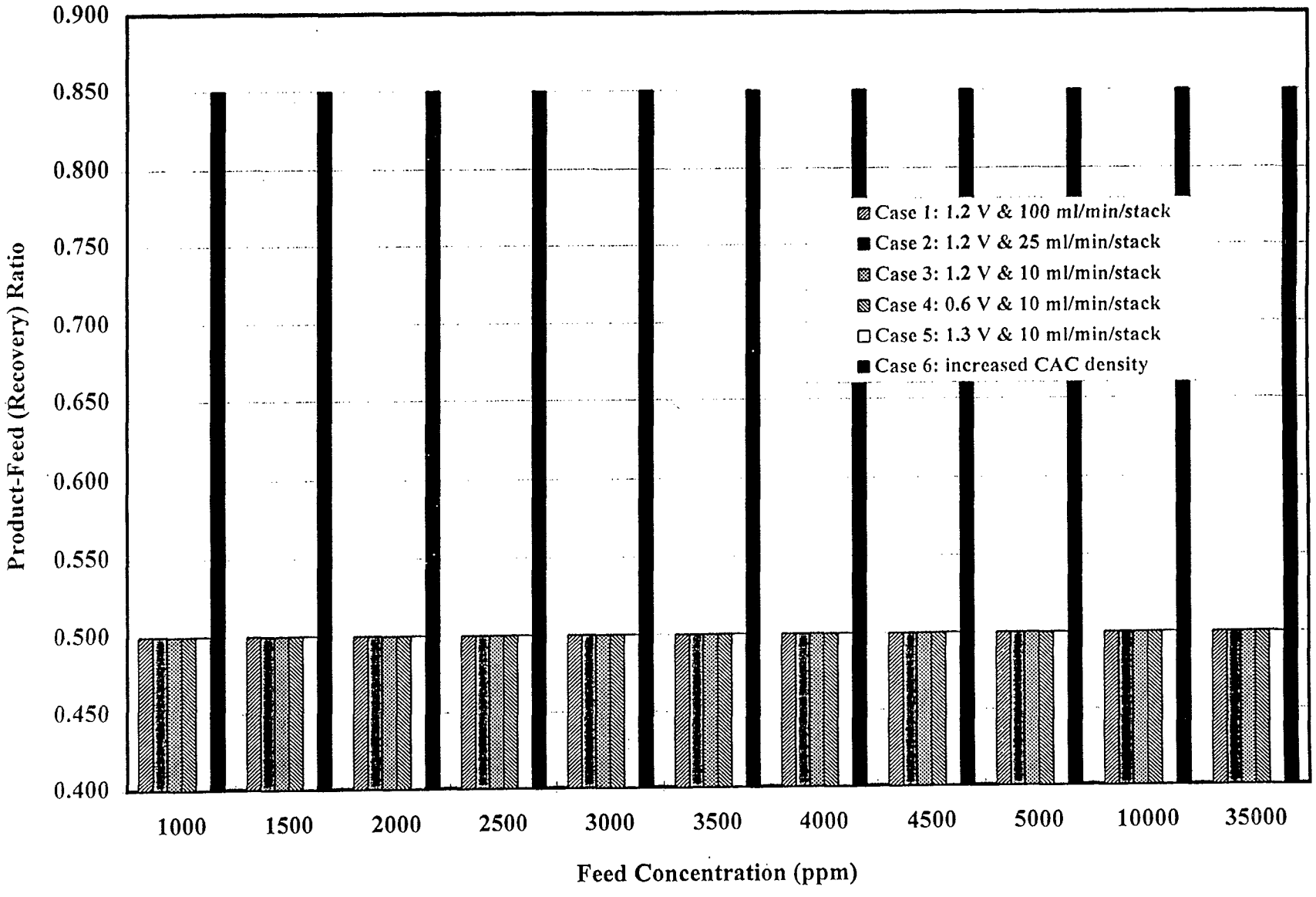
0.900
0.850
0.800
0.750
0.700
0.650
0.600
0.550
0.500
0.450
0.400
Product-Feed (Recovery) Ratio
Case 1: 1.2 V & 100 ml/min/stack
Case 2: 1.2 V & 25 ml/min/stack
Case 3: 1.2 V & 10 ml/min/stack
Case 4: 0.6 V & 10 ml/min/stack
Case 5: 1.3 V & 10 ml/min/stack
Case 6: increased CAC density
1000
1500
2000
2500
3000
3500
4000
4500
5000
10000
35000
Feed Concentration (ppm)

Figure 6a

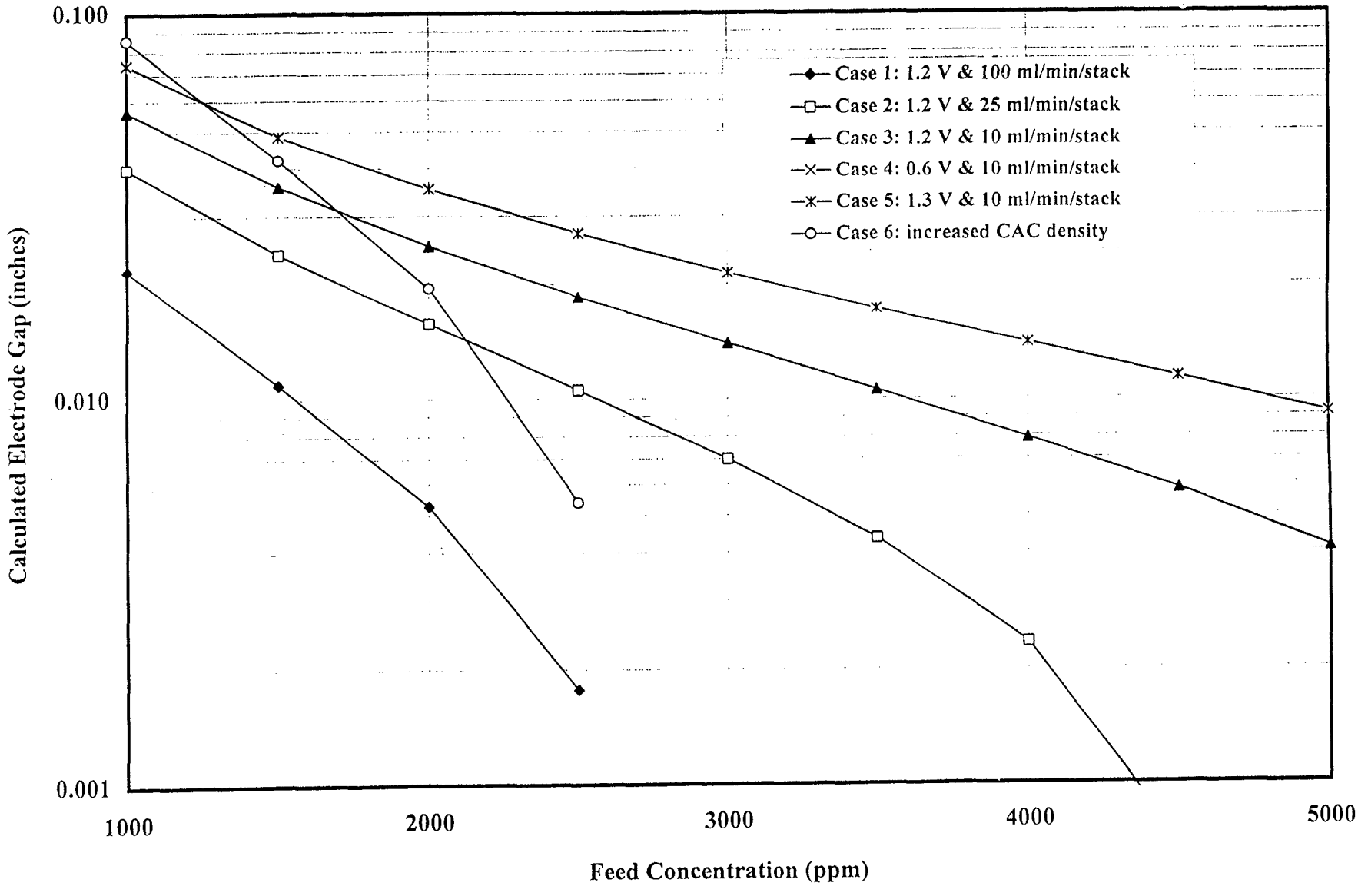
0.100
0.010
0.001
1000
2000
3000
4000
5000
Calculated Electrode Gap (inches)
Feed Concentration (ppm)
Case 1: 1.2 V & 100 ml/min/stack
Case 2: 1.2 V & 25 ml/min/stack
Case 3: 1.2 V & 10 ml/min/stack
Case 4: 0.6 V & 10 ml/min/stack
Case 5: 1.3 V & 10 ml/min/stack
Case 6: increased CAC density

Figure 6b

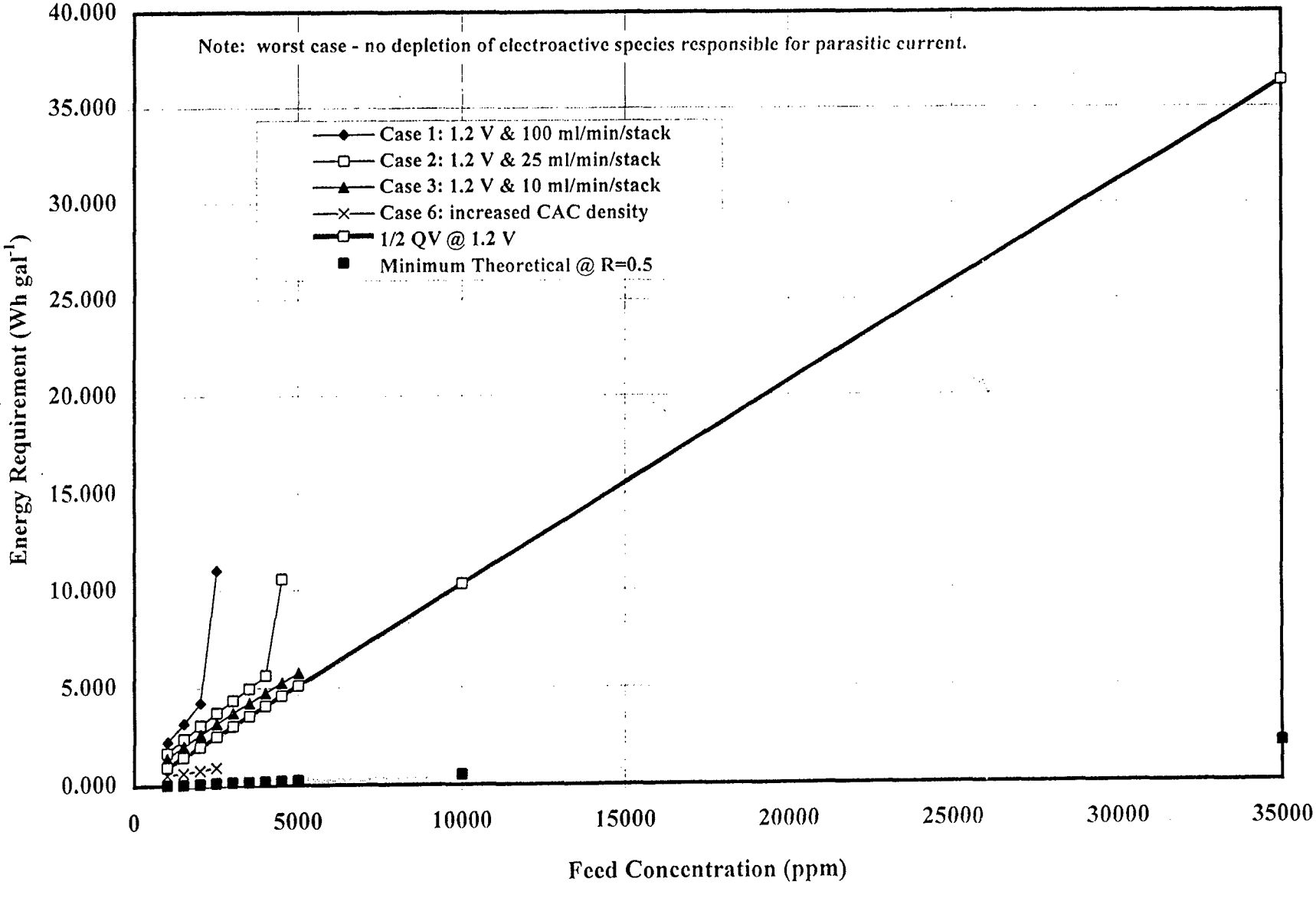
Note: worst case - no depletion of electroactive species responsible for parasitic current.
Case 1: 1.2 V & 100 ml/min/stack
Case 2: 1.2 V & 25 ml/min/stack
Case 3: 1.2 V & 10 ml/min/stack
Case 6: increased CAC density
1/2 QV @ 1.2 V
Minimum Theoretical @ R=0.5
Energy Requirement (Wh gal-1)
40.000
35.000
30.000
25.000
20.000
15.000
10.000
5.000
0.000
0
5000
10000
15000
20000
25000
30000
35000
Feed Concentration (ppm)

Figure 6c

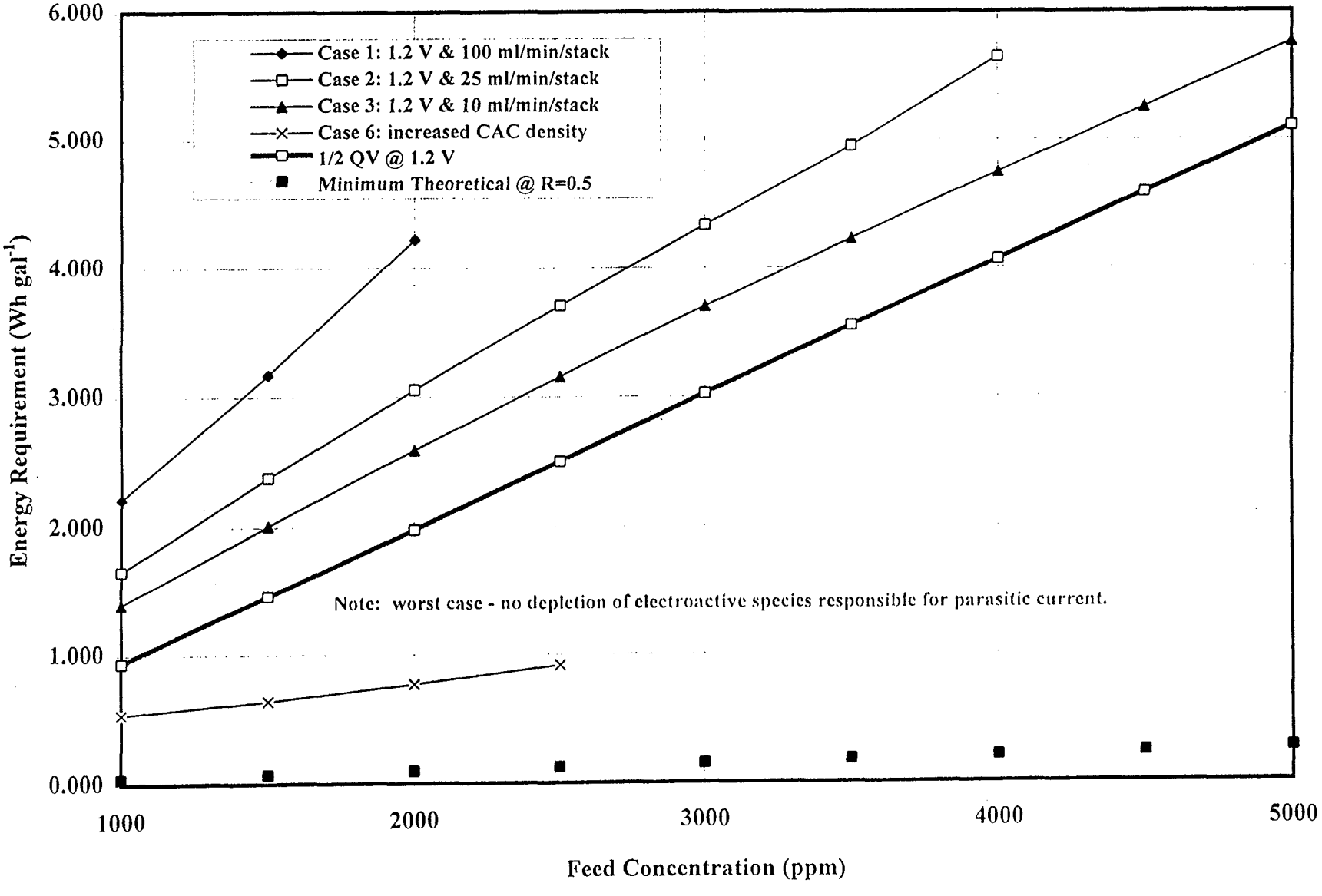
6.000
5.000
4.000
3.000
2.000
1.000
0.000
Energy Requirement (Wh gal^{-1})
1000
2000
3000
4000
5000
Feed Concentration (ppm)
Case 1: 1.2 V & 100 ml/min/stack
Case 2: 1.2 V & 25 ml/min/stack
Case 3: 1.2 V & 10 ml/min/stack
Case 6: increased CAC density
1/2 QV @ 1.2 V
Minimum Theoretical @ R=0.5
Note: worst case - no depletion of electroactive species responsible for parasitic current.

Figure 6d

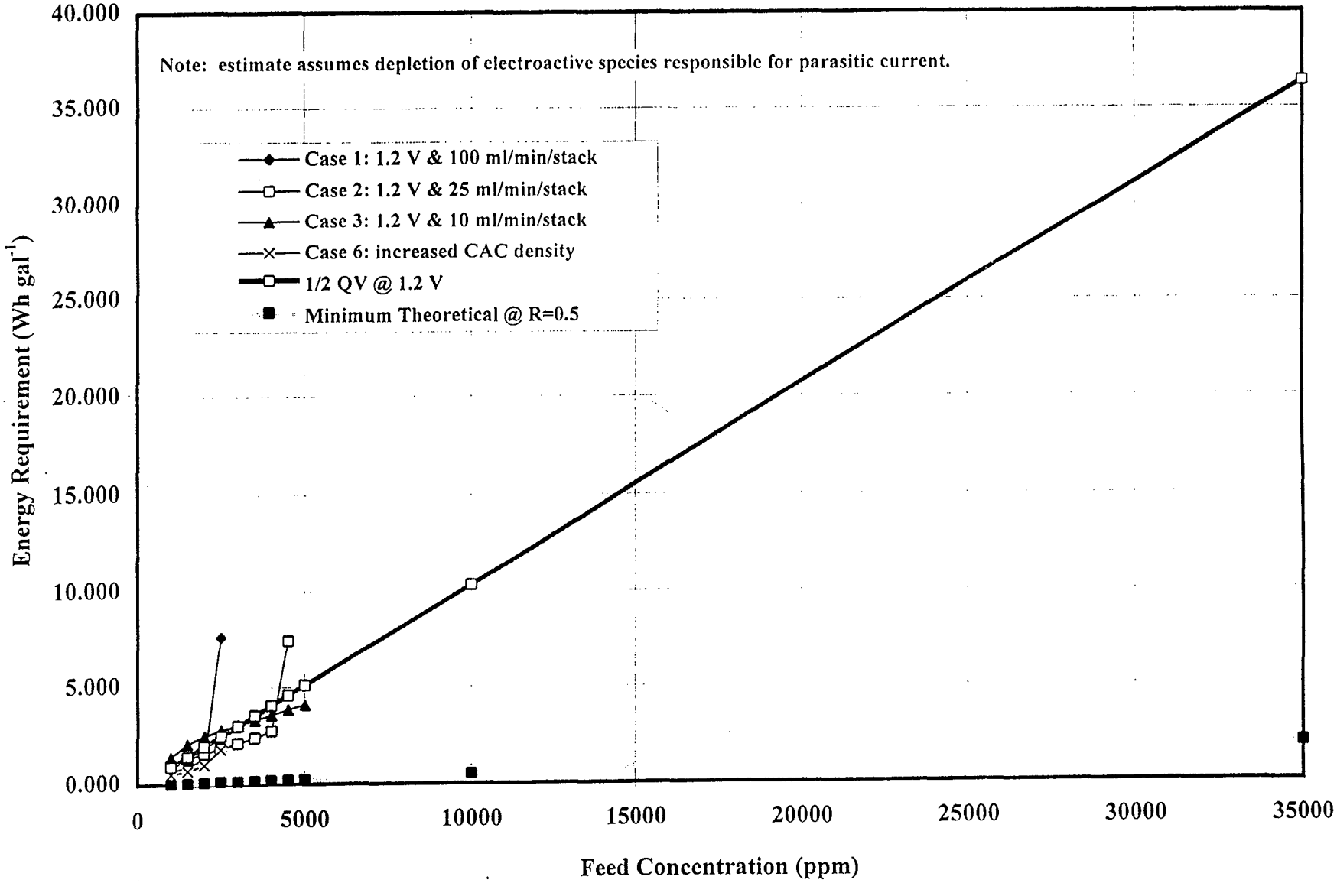
Note: estimate assumes depletion of electroactive species responsible for parasitic current.
Case 1: 1.2 V & 100 ml/min/stack
Case 2: 1.2 V & 25 ml/min/stack
Case 3: 1.2 V & 10 ml/min/stack
Case 6: increased CAC density
1/2 QV @ 1.2 V
Minimum Theoretical @ R=0.5
Energy Requirement (Wh gal-1)
40.000
35.000
30.000
25.000
20.000
15.000
10.000
5.000
0.000
0
5000
10000
15000
20000
25000
30000
35000
Feed Concentration (ppm)

Figure 6c

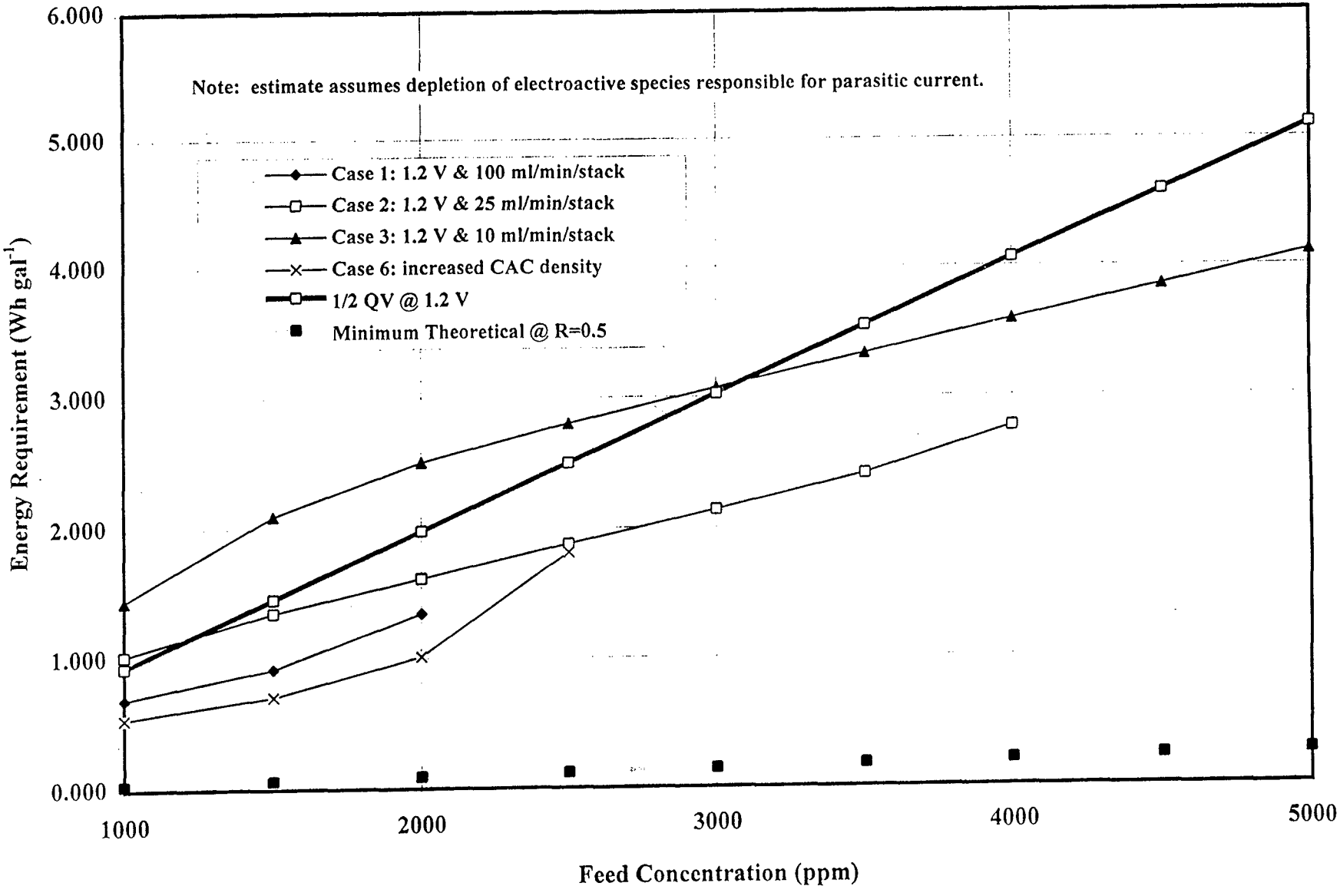
Note: estimate assumes depletion of electroactive species responsible for parasitic current.
Case 1: 1.2 V & 100 ml/min/stack
Case 2: 1.2 V & 25 ml/min/stack
Case 3: 1.2 V & 10 ml/min/stack
Case 6: increased CAC density
1/2 QV @ 1.2 V
Minimum Theoretical @ R=0.5
Energy Requirement (Wh gal-1)
6.000
5.000
4.000
3.000
2.000
1.000
0.000
1000
2000
3000
4000
5000
Feed Concentration (ppm)

Figure 6f

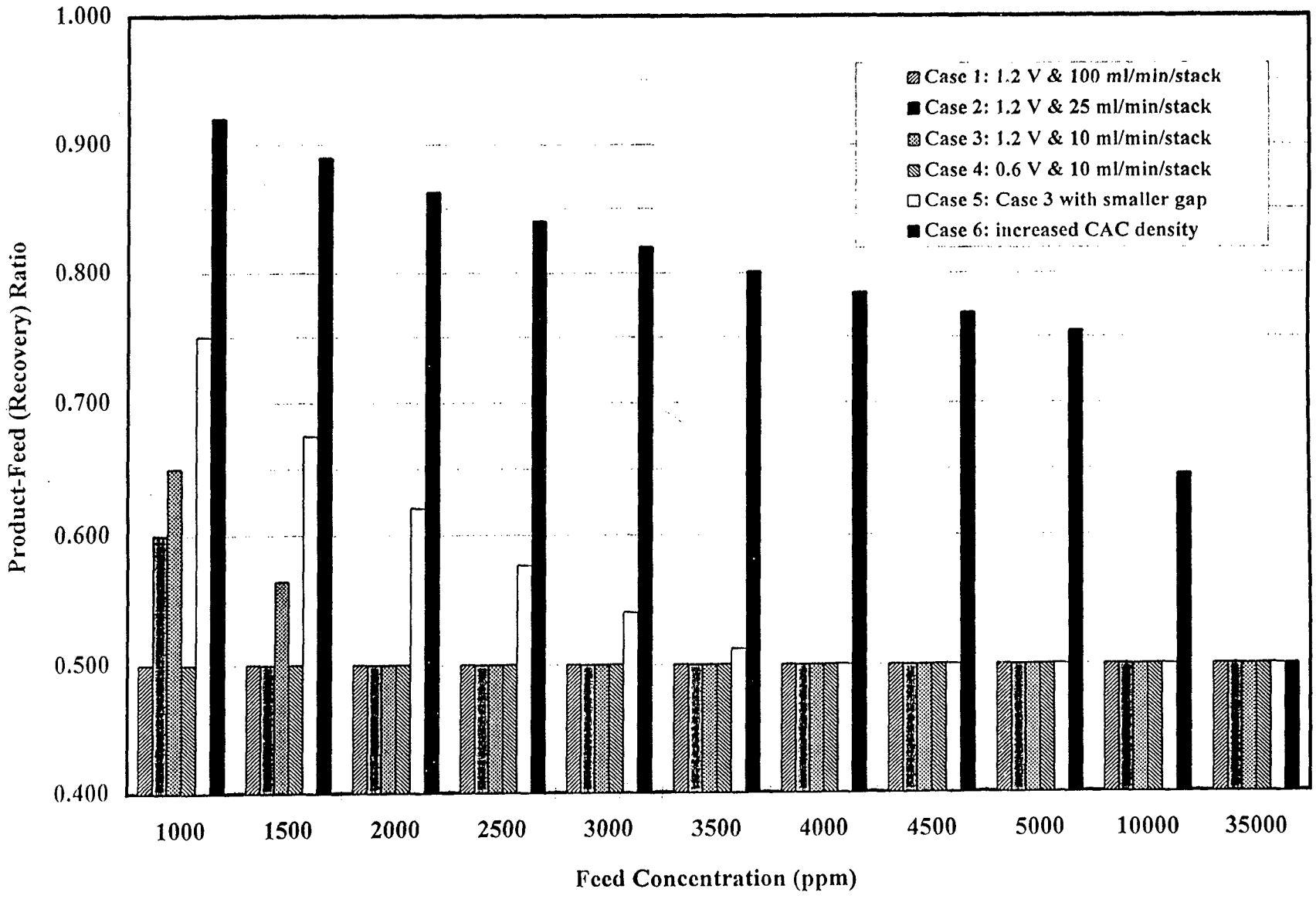
1.000
0.900
0.800
0.700
0.600
0.500
0.400
Product-Feed (Recovery) Ratio
Case 1: 1.2 V & 100 ml/min/stack
Case 2: 1.2 V & 25 ml/min/stack
Case 3: 1.2 V & 10 ml/min/stack
Case 4: 0.6 V & 10 ml/min/stack
Case 5: Case 3 with smaller gap
Case 6: increased CAC density
1000
1500
2000
2500
3000
3500
4000
4500
5000
10000
35000
Feed Concentration (ppm)

Figure 7a

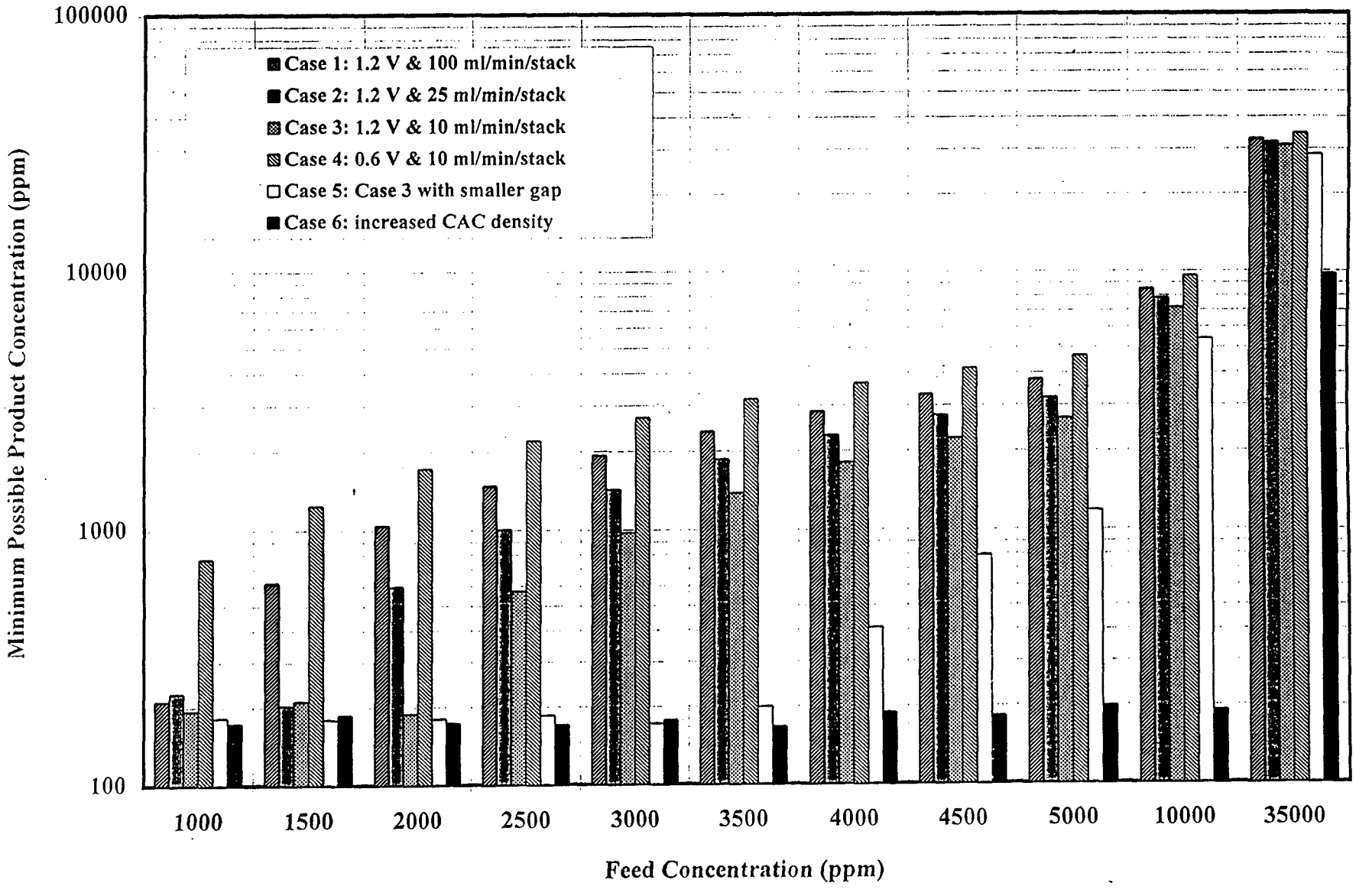
Case 1: 1.2 V & 100 ml/min/stack
Case 2: 1.2 V & 25 ml/min/stack
Case 3: 1.2 V & 10 ml/min/stack
Case 4: 0.6 V & 10 ml/min/stack
Case 5: Case 3 with smaller gap
Case 6: increased CAC density
Minimum Possible Product Concentration (ppm)
100000
10000
1000
100
1000
1500
2000
2500
3000
3500
4000
4500
5000
10000
35000
Feed Concentration (ppm)

Figure 7b

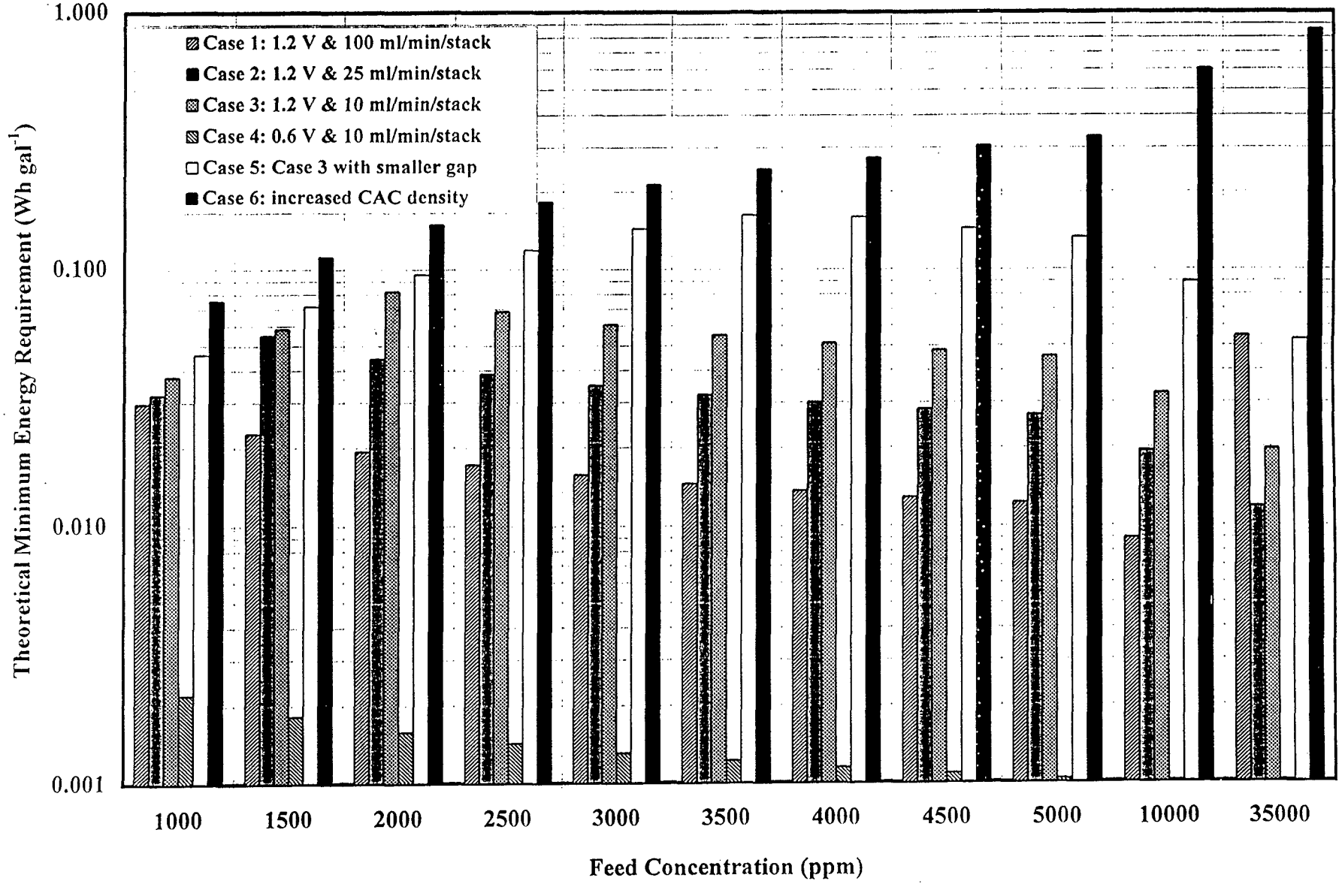
Case 1: 1.2 V & 100 ml/min/stack
Case 2: 1.2 V & 25 ml/min/stack
Case 3: 1.2 V & 10 ml/min/stack
Case 4: 0.6 V & 10 ml/min/stack
Case 5: Case 3 with smaller gap
Case 6: increased CAC density
1.000
0.100
0.010
0.001
Theoretical Minimum Energy Requirement (Wh gal-1)
1000
1500
2000
2500
3000
3500
4000
4500
5000
10000
35000
Feed Concentration (ppm)

Figure 7c

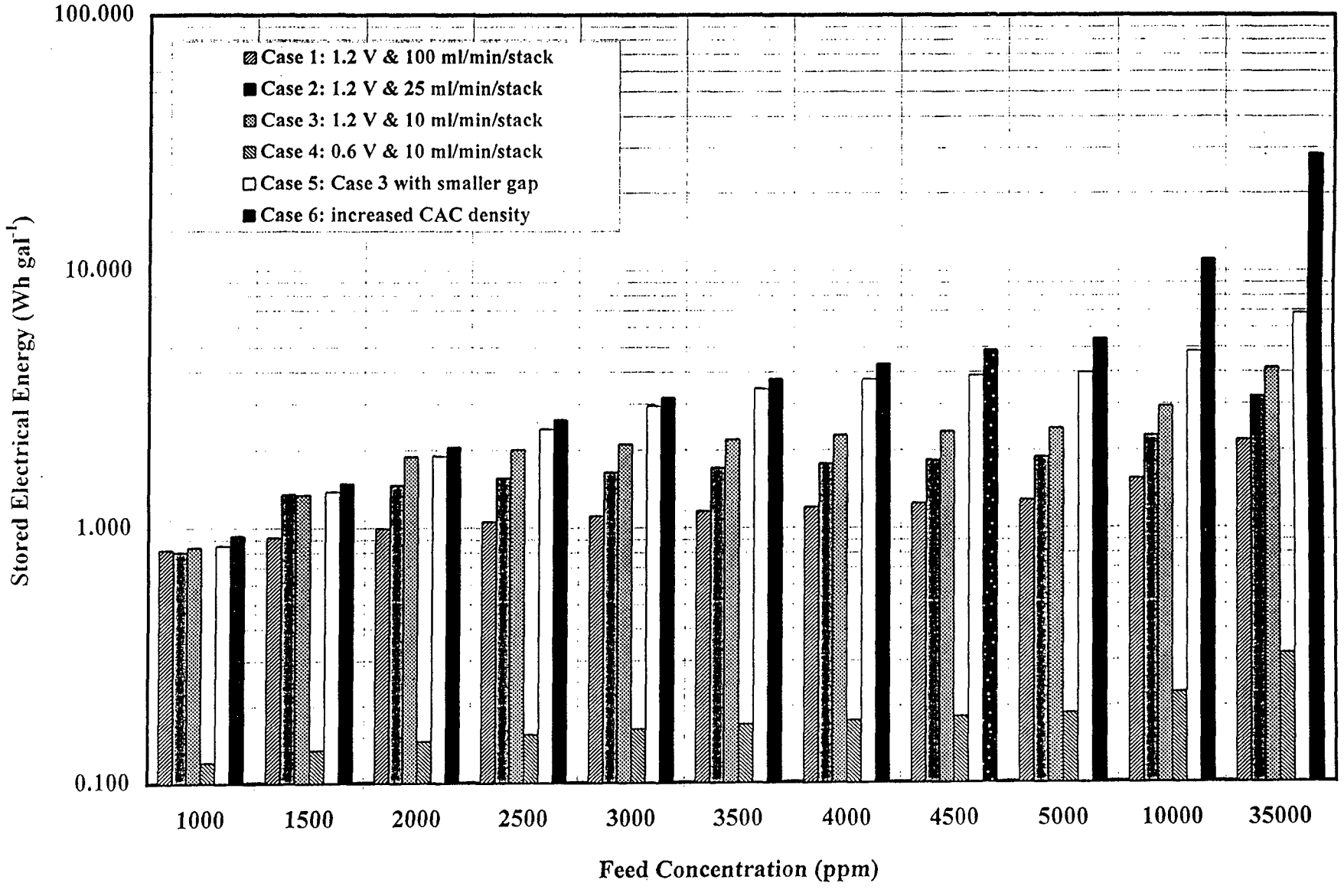
100.000
10.000
1.000
0.100
Stored Electrical Energy (Wh gal^{-1})
Case 1: 1.2 V & 100 ml/min/stack
Case 2: 1.2 V & 25 ml/min/stack
Case 3: 1.2 V & 10 ml/min/stack
Case 4: 0.6 V & 10 ml/min/stack
Case 5: Case 3 with smaller gap
Case 6: increased CAC density
1000
1500
2000
2500
3000
3500
4000
4500
5000
10000
35000
Feed Concentration (ppm)

Figure 7d

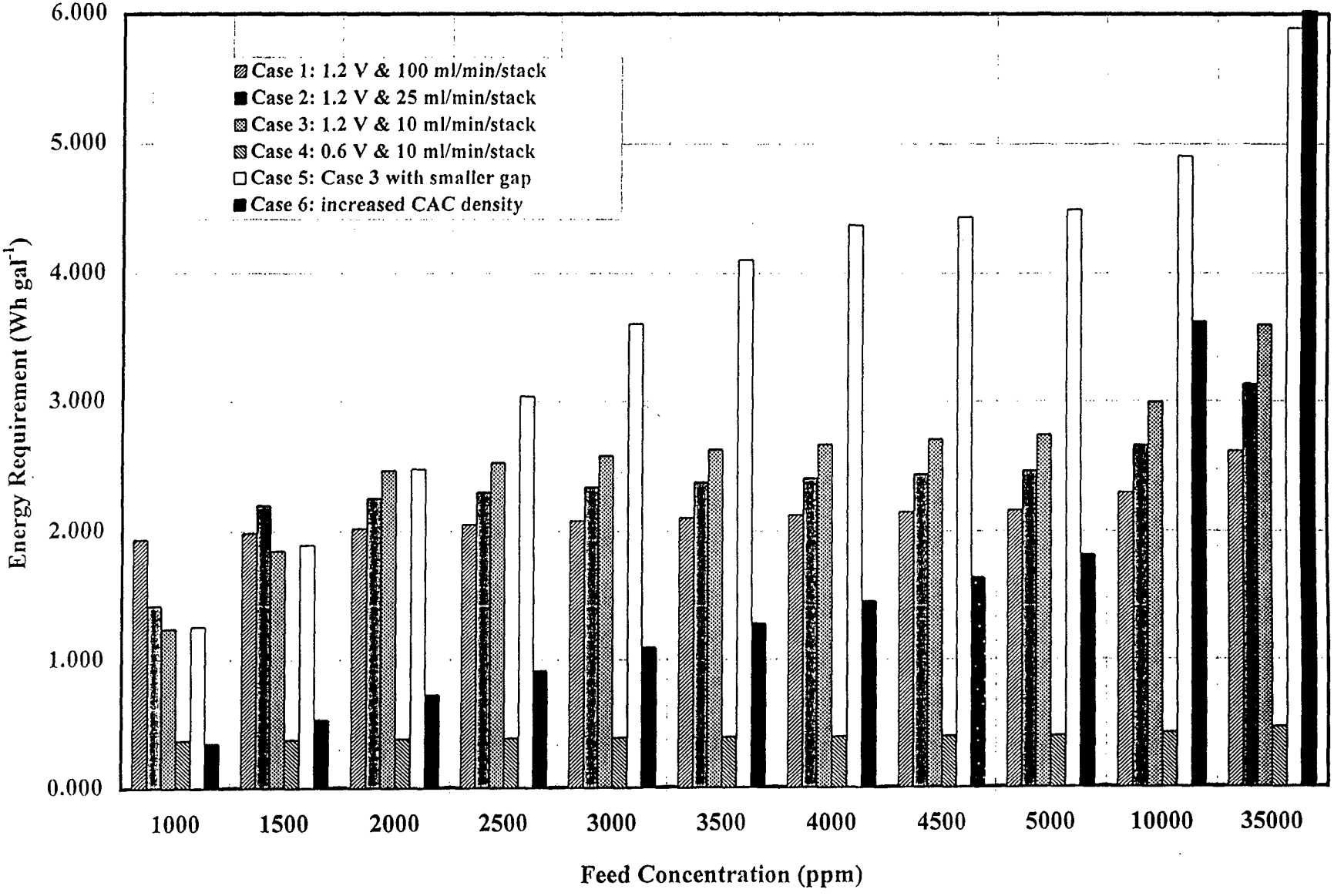
Case 1: 1.2 V & 100 ml/min/stack
Case 2: 1.2 V & 25 ml/min/stack
Case 3: 1.2 V & 10 ml/min/stack
Case 4: 0.6 V & 10 ml/min/stack
Case 5: Case 3 with smaller gap
Case 6: increased CAC density
Energy Requirement (Wh gal-1)
6.000
5.000
4.000
3.000
2.000
1.000
0.000
1000
1500
2000
2500
3000
3500
4000
4500
5000
10000
35000
Feed Concentration (ppm)

Figure 7c

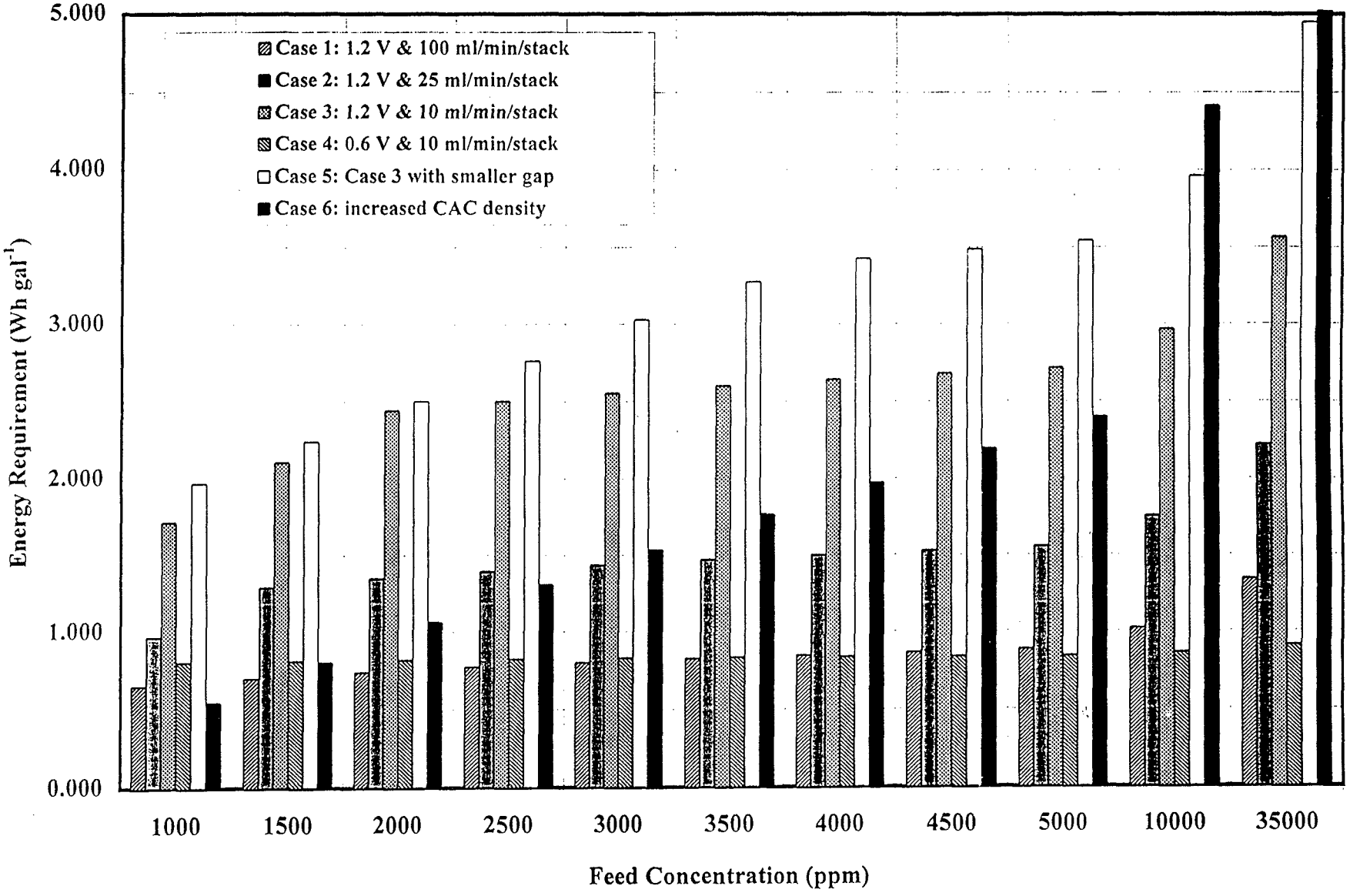
5.000
4.000
3.000
2.000
1.000
0.000
Energy Requirement (Wh gal^{-1})
Case 1: 1.2 V & 100 ml/min/stack
Case 2: 1.2 V & 25 ml/min/stack
Case 3: 1.2 V & 10 ml/min/stack
Case 4: 0.6 V & 10 ml/min/stack
Case 5: Case 3 with smaller gap
Case 6: increased CAC density
1000
1500
2000
2500
3000
3500
4000
4500
5000
10000
35000
Feed Concentration (ppm)

Figure 7f.